Airborne Disease Transmission via Bioaerosols: Formation Mechanisms and the Influence of Viscoelasticity

Professor David Weitz Matthew K. Thomas

Airborne disease transmission via bioaerosols: Formation mechanisms and the influence of viscoelasticity

Abstract

Airborne disease transmission is a prominent problem facing an increasingly mobilized world. It involves small droplets (bioaerosols) containing pathogens which form in the lungs and are expelled to the environment, where they may persist in the air until inhaled by others. Conceptually, there are two basic approaches to preventing transmission: protect the potential target, or eliminate the source. To this end, the effectiveness of modifying mucus viscoelasticity, through cation exposure, to prevent pathogen transport via bioaerosols was investigated.

In vitro models were developed to explore the proposed mechanisms for droplet formation: shear-induced surface-wave instabilities in the airway lining fluid (ALF) of the upper airways; and film formation during the re-opening of collapsed bronchioles in the lower airways. Droplet formation during tidal breathing was shown to be an inhalation process for both upper and lower airway models, and the bifurcation angle of the first bronchi was relevant to the upper airway model. A simulated cough system was also developed and produced the largest number of droplets.

COPD sputum viscoelasticity was characterized and its response to cation presence measured: low concentrations of calcium resulted in increased complex modulus and decreased loss tangent (indicating increased fluid stiffness resulting from higher elasticity). Higher

concentrations of calcium had the reverse effect. Using the cough system, calcium treated (low concentration) and untreated sputum were compared: treated sputum produced fewer droplets. Droplet concentration (number per liter of air) correlated well with the magnitude of the complex modulus.

Once the reduction in total droplets was established, pathogen transport experiments, in which human rhinovirus (HRV) was added to calcium-treated and untreated COPD sputum, were performed. Cell culture media was exposed to cough-air from the samples and then placed on HRV-sensitized HeLa cells, which were then monitored for cell death. Cell death was observed for untreated sputum samples, but not for cation-treated samples, indicating that reducing bioaerosol formation (through cationic modification of mucus viscoelasticity) prevented airborne transport of the virus.

Table of Contents

Acknowledgements

No great endeavor is performed in complete isolation, and this work is no different: it would not have been possible but for the support of many others. In particular, I would like to thank David Edwards of Harvard University, Robert Clarke and Jean Sung of Pulmatrix, Inc. and above all my wife, Jenny Thomas.

Chapter 1: Airborne infectious disease transmission

Introduction:

Transmissible diseases are a basic part of existence. They occur in many forms and varieties, but the most basic description would involve an invasive and foreign particle entering a host and replicating, typically to the detriment of the host. There are many routes or vectors which a particle can take to enter the body – for example, it may directly enter the bloodstream through cuts or other wounds, or it may colonize the gastrointestinal or pulmonary tracts after being swallowed or inhaled – the exact mechanism of infection will depend on the specific pathogen. However, the simple fact that, before an infection can begin, a pathogenic organism must first reach its target destination makes preventing exposure an immediate and obvious route to halting the spread of these infectious diseases.

At the simplest level, this can be accomplished in one of two ways: either creating "barriers" around the destination, or preventing the pathogen from escaping from the source. The former is frequently employed through the use of masks, gloves, antibacterial sprays and washes but it remains a passive defense which does not always eliminate the pathogen from the environment. It thus becomes only a question of time until the "barrier" is circumvented (through mistakes, negligence, ineffectiveness or even adaptation).As long as the pathogen is in the environment, the risk of infection remains. Targeting the source is therefore more desirable, however it is also more difficult – pathogens are transported within bodily fluids (blood, mucus, etc.) and are shed from the body in a variety of ways, many of which are invisible to the naked eye. Furthermore, the exact route to infection is not uniform across all pathogens.

Respiratory disease and transmission:

Of particular interest are respiratory diseases, as these infections can rapidly spread to large populations through airborne transmission (which involves the spread of pathogens through expelled droplets produced by talking, breathing, coughing or sneezing), potentially reaching global proportions. Over the past decade there have been a number of pulmonary diseases that created widespread panic with the fear of pandemic. These include severe acute respiratory syndrome (SARS, 2003); avian flu (H5N1, 2004 and 2005, although airborne transmission was not observed and subsequent studies have shown limited human-to-human transmission[1]); and more recently swine flu (H1N1, 2008). These epidemics generated major headlines and highlighted the seriousness (and often hysteria) which are associated with the threat of pandemics. Airborne transmission can also occur in many other respiratory diseases, including seasonal influenza, the common cold (rhinovirus), pulmonary tuberculosis (TB), measles, chicken pox, pneumonia and anthrax, amongst others.

Figure 1.1: Droplet spray visualization

In 2004 a study conducted on the SARS outbreak in Hong Kong and published in the New England Journal of Medicine by Ignatius Yu et al.[2] concluded that airborne transmission was the likely route for the spread of the virus. Chad Roy (U.S. Army Medical Research Institute of Infectious Diseases) and Donald Milton (Harvard School of Public Health) cited Yu's study in an article[3] in the same publication to highlight the need for a fundamental shift in how doctors understood and approached the relationship between infectious disease and airborne transmission. Claiming the traditionally held view that diseases either were "true" airborne infections or not airborne infections at all was too limited, and did not lead to "useful thinking" about the problem, they proposed a new classification system for airborne diseases as "obligate, preferential, or opportunistic." Obligate airborne diseases transmit only through aerosols; preferential airborne diseases transmit primarily via aerosols, but may spread in other ways as well (such as direct contact); opportunistic airborne diseases may transmit via aerosol, but primarily spread through other means.

Roy and Milton pointed out the need for a deeper understanding of airborne transmission, specifically in regards to hospitals and other indoor settings (schools, airplanes, etc.) while citing the transmission of SARS in hospital waiting rooms. They believed their new categorization system would provide a more nuanced way of thinking about disease transmission, specifically in regards to prevention. For example, in preferential or opportunistic airborne disease scenarios, hand-washing alone might reduce the probability for transmission, but it would not eliminate it – a combination of preventative measures would be necessary – but due to observed decreases in transmission, the additional measures might not be implemented. Furthermore, some measures thought to reduce bioaerosol transmission, such as the use of surgical masks, have been shown to

be ineffective for any but the largest droplets[4]. Hence, further research into airborne disease transmission and prevention is vital.

Historically, airborne transmission has been thought to be the result of pathogen-laden, large-diameter droplets expelled via coughing, sneezing or talking. In the 1940s, J. P. Duguid (Edinburgh University) performed a series of experiments attempting to clarify the role of droplet spray in infection transmission[5]. Patients with a confirmed infection of either haemolytic streptococcus, diphtheria or tuberculosis were asked to perform different breathing maneuvers (coughing, sneezing, talking) while a microscope slide or culture plate was held in front of them to collect expelled droplets by impingement. The slide or plate was then analyzed for pathogen presence. The study acknowledged that only the largest droplets would be collected on the plates, but claimed that the majority of "pathogenic organisms were contained in the large droplets." This claim was made without reference to any supporting evidence, and reflects the prevailing opinions of the time. These opinions were the result of a simple fact: there were no methods for detecting smaller droplets (aerosols), and therefore no one was aware of how many were being produced. With the development and proliferation of optical methods for measuring small and very small airborne particles (nanometers to microns in scale) in the 1980s and 1990s, research began on the size and number of expelled droplets.

In 1997, R. Papineni and F. Rosenthal (Purdue University) published a study on the number and size distribution of droplets in the exhaled breath of healthy humans[7]. Not only did they confirm the presence of small droplets (less than 5 microns in diameter), but they found that these droplets were present in numbers that were significantly greater than those of larger droplets (more than an order of magnitude difference).

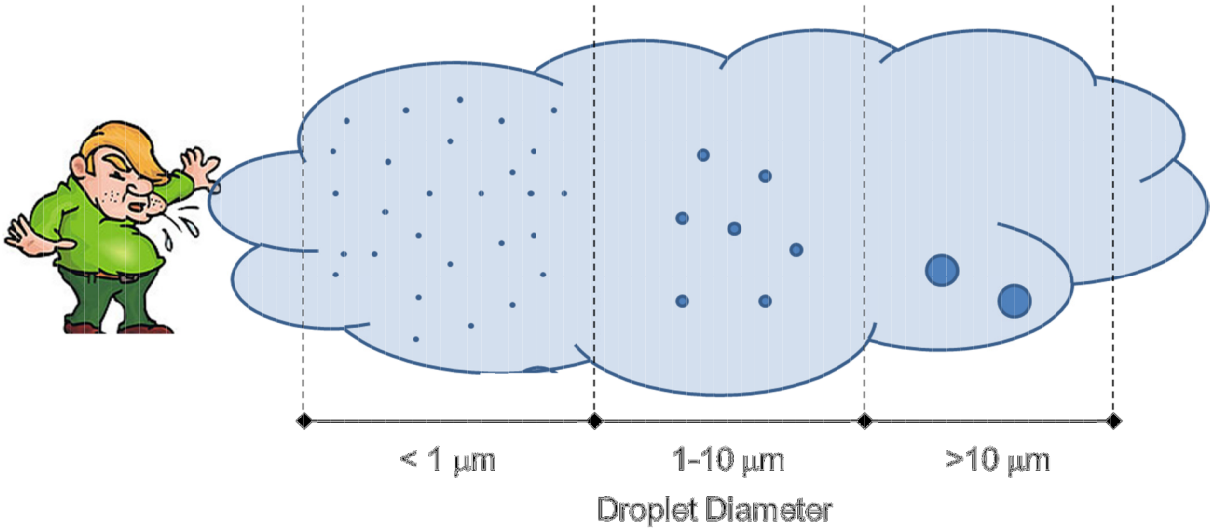

Figure 1.2: Expelled droplets – the number of droplets released increases dramatically as the size decreases, however this was not observed until the 1990s, after the development of optical particle counting techniques.

Given that the size of nearly all viruses and many bacteria are microns or less (rhinovirus, for example, is only 30 nanometers in diameter), they could easily be contained within the expelled aerosols. This meant that it was not only possible, but highly probable that the majority of expelled pathogens were to be found in the smaller droplets, based simply on the sheer number produced. Pathogen-laden aerosols (bioaerosols) are a greater threat compared to large droplets because they may persist in the environment for longer and may travel further from the source, placing a larger population at risk of infection, especially in public spaces. As a result of Papineni and Rosenthal's study, research on airborne disease transmission began to give increased consideration to bioaerosols, although practical prevention efforts reflecting that research have lagged (as evidenced by Roy and Milton's desire to encourage "useful thinking" by introducing new categories to describe airborne disease transmission following the SARS outbreaks).

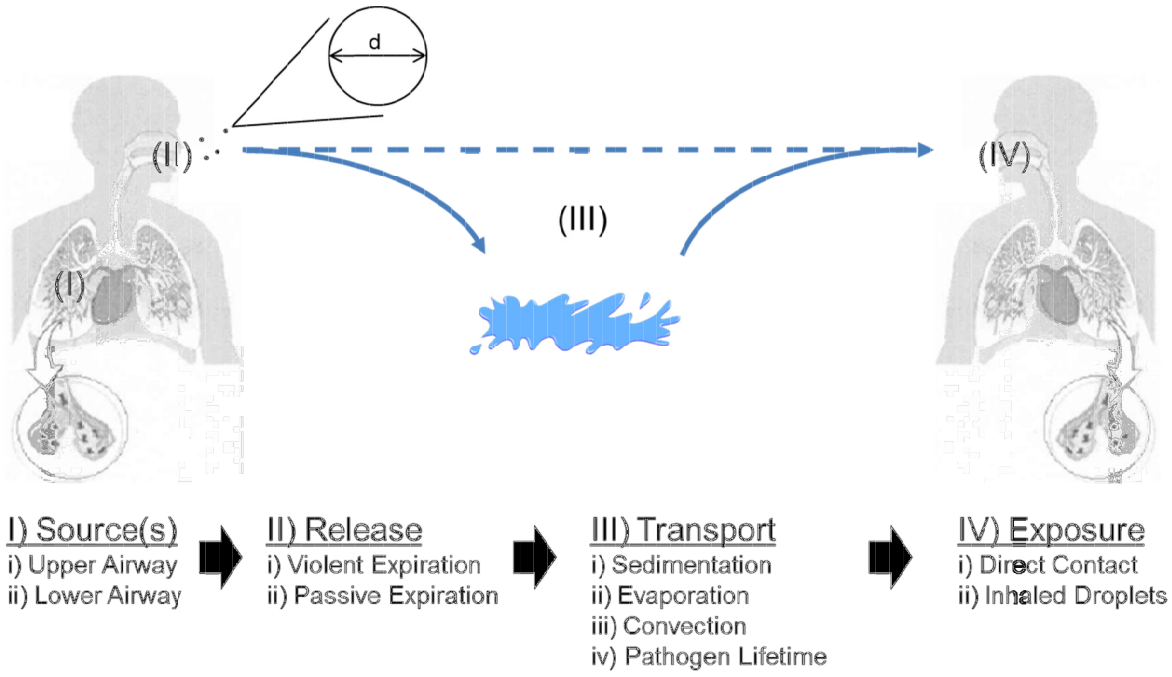

Figure 1.3: Stages of airborne transmission, including small and large droplets

Airborne transmission and prevention:

Airborne transmission can be broken into 4 major stages, as shown in Figure 1.3. In stage I, droplets are formed at the infection site within the pulmonary system. They are then transported to the naso-pharyngeal region and expelled to the environment in stage II. The droplets range in size and number, but are loosely divided into large droplets and small droplets (bioaerosols). The majority of bioaerosol research has, to date, focused on this stage by looking at the number, size and composition of expelled droplets. Once in the environment, they are subject to numerous forces resulting from environmental conditions, the droplet composition and its size. Stage III encompasses these forces, in which the droplets are subject to sedimentation, evaporation (in which larger droplets may transition to smaller droplets if evaporation occurs rapidly enough) and convective transport. The length of time the droplets persist in the environment is a function of the exact conditions they are exposed to, as is the length of time

pathogens remain infectious (i.e. pathogen lifetime). Droplets which settle will contaminate nearby surfaces, whereas bioaerosols persist in the air and may be convectively transported larger distances. Both these routes can lead to exposure (stage IV), either through contact with contaminated surfaces or through inhaled bioaerosols depositing directly in the lungs.

Prevention methods have largely focused on stage III and IV, either through treating the environment (washing hands, cleaning exposed surfaces, etc.) or erecting barriers to prevent inhalation (i.e. facemasks). However in 2004, David Edwards (Harvard University) et al. published a study in the Proceedings of the National Academy of Science[8] in which they screened healthy human subjects for exhaled droplets both before and after treatment with nebulized isotonic saline. This novel approach sought to address the issue of airborne transmission by targeting the bioaerosol origin (stage I). They identified a portion of the population as "super-producers" – individuals who expelled significantly greater droplet amounts compared to the rest of the population. Treatment of these individuals with nebulized saline subsequently reduced the number of droplets they expelled. These results were replicated with Holstein bull calves in a subsequent study (R. Clarke et al., 2005, American Journal of Infection Control[10]). Further investigation of this effect was carried out by W. Watanabe et al. (2007, Journal of Colloid and Interface Science)[9] and indicated that inhaled salt water altered the viscoelasticity of airway mucus through mucin charge-shielding, thereby stabilizing the interface and resulting in reduced droplet formation.

Debate has arisen over the location and mechanism of bioaerosol formation within the pulmonary system. The pulmonary system (Figure 1.4) is commonly divided into two regions: the upper airways (which consists of the naso-pharynx, trachea, and bronchi) and the lower airways (bronchioles and alveoli)[14].While the traditional view has been that droplets are formed

through shear forces acting on the surface of the airway lining fluid in the upper airways (as demonstrated computationally by J. Moriarty and J. Grotberg in their 1999 publication)[11], an alternative method involving film rupture in the lower airways has also been proposed (with supporting research performed by G. Johnson and L. Morawska published in 2009 and 2010)[12,13].As the two mechanisms differ significantly, the relevant physical properties are likely to differ as well; hence any investigation into bioaerosol prevention must consider both of these approaches.

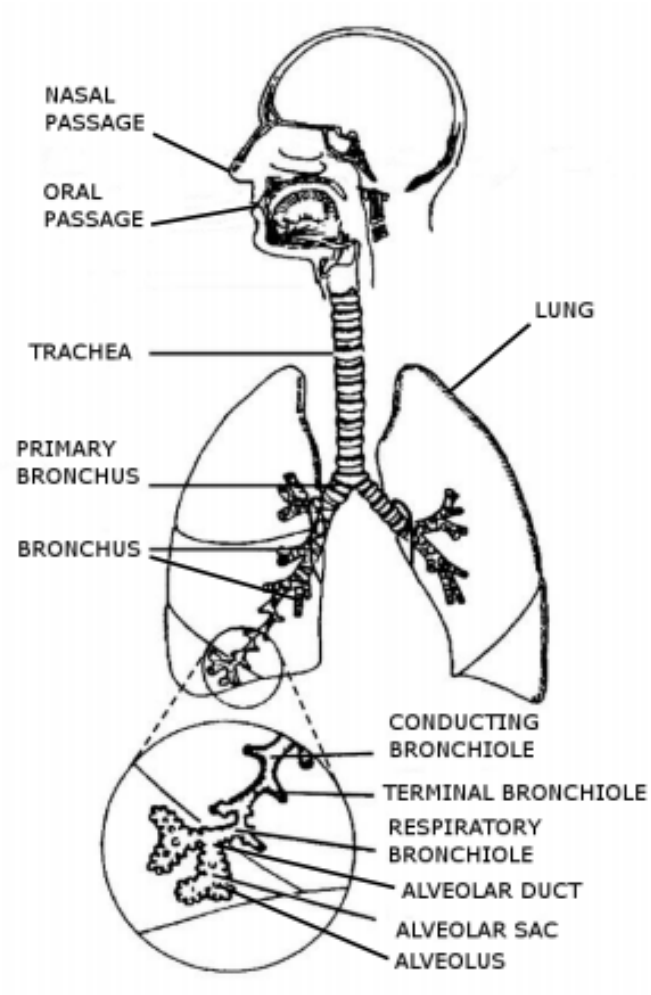

Figure 1.4: The pulmonary system[14]

Thesis research:

The purpose of my thesis will be to investigate the small droplet hypothesis of airborne disease transmission (which states that small aerosols generated in the airways and expelled to the environment can contain pathogens which lead to infection when inhaled), particularly with the aim of preventing such transmission by targeting droplet origins (specifically through the use of cationic agents to alter the physical properties of airway mucus). These goals will be accomplished by empirical examination of the following hypotheses, which were developed based on literature review and empirical results (to be demonstrated in subsequent chapters):

i) Droplet generation during tidal breathing can occur in both the upper airways (via surface shear) and lower airways (via film rupture) during inhalation, and will vary with bifurcation angle in the upper airways.

ii) Mucus viscoelasticity will influence droplet formation by shear forces, with increased stiffness yielding fewer droplets in total.

iii) Reducing the number of bioaerosols generated decreases the probability of airborne pathogen transport, and therefore the transmission of infection.

This research will yield a deeper understanding of bioaerosol formation and airborne disease transmission. It will clarify the influence of cations on mucus viscoelasticity, and provide guidelines regarding cation concentration which will have applicable ramifications in determining effective dosages. Finally, bench-top tools will be developed to enable more rapid experimentation on the mechanisms of bioaerosol formation.

References:

1. Ungchusak, K.; Auewarakul, P.; Dowell, S.; Kitphati, R.; Auwanit, W.; Puthavathana, P.; Uiprasertkul, M.; Boonnak, K.; Pittayawonganon, C.; Cox, N.; Zaki, S.; Thawatsupha, P.; Chittaganpitch, M.; Khontong, R; Simmerman, J.; Chunsutthiwat, S. (2005) *N. Engl. J. Med.* 352:333-340
2. Yu, I.; Li, Y.; Wong, T.; Tam, W.; Chan, A.; Lee, J.; Leung, D.; Ho, T. (2004) *N. Engl. J. Med.* 350:1731-1739
3. Roy, C.; Milton, D. (2004) *N. Engl. J. Med.* 350:1741-1744
4. Charney, W. (1991) *J. Occu. Med.* 33(9): 943-944
5. Duguid, J. (1946) *British Medical Journal* 265-268
6. Loudon, R.; Roberts, R. (1967) *American Review of Respiratory Disease*95(3): 435-438
7. Papineni, R.; Rosenthal, J. (1997) *J Aerosol Med.* 10(2):105-116
8. Edwards, D.; Man, J.; Brand, P.; Katstra, J.; Sommerer, K.; Stone, H.; Nardell, E.; Scheuch, G. (2004)*PNAS* 101(50): 17383-17388
9. Watanabe, W.; Thomas, M.; Clarke, R.; Klibanov, A.; Langer, R.; Katstra, K.;Fuller, G.; Griele, L.; Fiegel, J.; Edwards, D. (2007) *J Colloid Interface Sci.* 307(1): 71–78
10. Clarke, R.; Katstra, J.;Man, J.;Dehaan, W.;Edwards, D.;Griel, L. (2005)*American J Infection Control*33(5): 85
11. Moriarty, J.; Grotberg, J. (1999) *J. Fluid Mech*. 397: 1–22.
12. Johnson, G.; Morawska, L. (2009) *J Aerosol Med Pulm Drug Deliv*. 22:1-9.
13. Morawska, L.; Johnson, G.; Ristovski, Z.; Hargreaves, M.; Mengersen, K.; Corbett, S.; Chao, C.; Li, Y.; Katoshevski, D.(2009) *J Aerosol Sci.* 40:256-269
14. Hinds, W.(1982) *Aerosol technology - properties, behaviour, and measurements of airborne particles*

Chapter 2: Mechanisms of bioaerosol formation and transport

Introduction:

In order to investigate airborne transmission through bioaerosols, as discussed in chapter 1, a review of existing literature and theory regarding the mechanisms of formation and transport is necessary. Bioaerosols (biological aerosols) are small, airborne droplets containing pathogens and other biological material which are generated in the lungs[1]. They are formed from the airway lining fluid (ALF) which is a protective coating covering the entire pulmonary system. As such, the material properties of the ALF will influence the mechanics of droplet formation. The structure of the pulmonary system will also be relevant, especially in regards to the type of breath-action (coughing versus tidal breathing) as well as the location of droplet formation.

Some controversy over the exact mechanism and origin of droplet formation has arisen over the past decade, particularly with respect to formation during tidal breathing, resulting in two major schools of thought. The first states that droplet generation occurs in the upper airways due to shedding (arising from instabilities) from surface wave-crests formed in the ALF as the result of surface-shearing by air. This mechanism is similar to that involved in cough-generated droplets, but occurs at much lower air-flow velocities. Kelvin-Helmholtz instabilities arising from core-annular flow were studied experimentally by I. Kataoka in 1982[26], and droplet formation was shown to be theoretically possible for a complete ALF model by J. Moriarty and J. Grotberg in 1999[18]. The second mechanism proposed involves droplet shedding from ruptured films which arise from the reopening of collapsed bronchioles in the lower airways. The basic mechanism of film rupture producing droplets was first reported by Blanchard in 1963 with respect to bubbles in sea water[27]. Small-airway collapse in healthy subjects was established in the 1970s (L. Engel et al. demonstrated the phenomenon in 1975[28]), but the link to film-rupture

and droplet generation was not suggested until 2009, when it was proposed by G. Johnson and L. Morawska[19].

The exact origin of bioaerosols remains an active area of investigation. The pulmonary environment and structure, including the properties of the ALF, form the starting point for any inquiry. Both mechanisms discussed above will be examined in greater detail, along with an analysis of the major forces acting on the droplets after they are formed.

Airway lining fluid and mucins:

The basic structure of the ALF is biphasic (Figure 2.1)[2], consisting of a viscoelastic (gel) upper layer and a serous (sol) sub-layer which act to protect the underlying epithelial cell layer (including goblet cells where mucins are formed). The overall thickness ranges from 5 to 100 microns – the exact thickness varies with health, hydration and location within the lungs[3], although the sol layer remains relatively invariable at 3 to 5 microns. The primary constituents of the ALF are water, proteins (surfactants and mucins) and salt-ions (sodium, potassium, calcium, magnesium, etc.). There is also a mixture of lipids, cells (macrophages) and other cellular matter, as well as environmental contaminants present (which are typically lodged within the mucus upper layer).

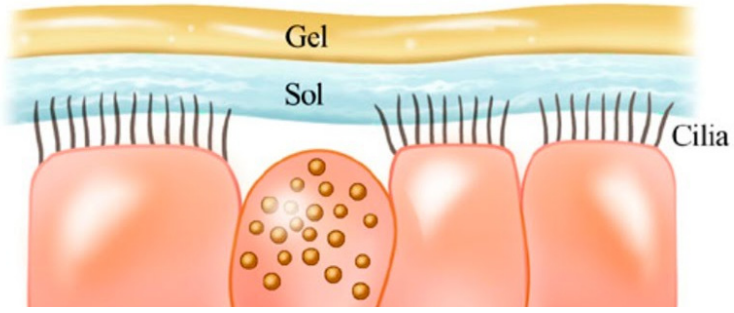

Figure 2.1: Basic schematic structure of the ALF coating the epithelial cell lining[4]

ALF is one of the lung's primary defense mechanisms[3], acting as a protective layer designed to trap or slow contaminants/pathogens and prevent access to the epithelial layer of the lungs, as well as maintain cellular hydration. These trapped contaminants are transported along with the ALF via the "mucociliary escalator"[5], which involves hair-like cilia extending from the epithelial layer through the sol sub-layer and moving in a two-stroke pattern (see Figure 2.2) in coordination with surrounding cilia. This process drives the ALF and any trapped material in a cephalic direction (towards the head), clearing the pulmonary system and exiting into the throat, where it can be swallowed and ultimately digested[5].

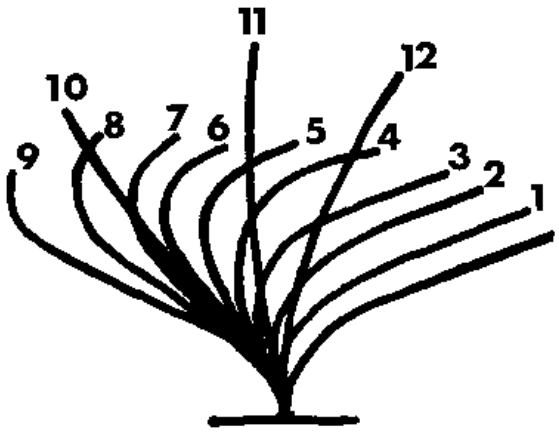

Figure 2.2: Ciliary two-stroke pattern – recovery stroke in limp state (1-9) followed by an effective stroke[6]

The hydration level of the ALF, which directly influences the thickness as well as other material properties, is primarily regulated by ion concentrations. Cellular ion channels sensitized to concentration trigger the secretion or absorption of aqueous fluid, which is thought to be released from serous and clara cells and absorbed by brush cells[7]. The basic constituents and their typical concentrations in healthy ALF are shown in Table 2.1 (data was taken from Junqueira's Basic Histology: Text and Atlas[8]).

Table 2.1: Mucus constituents and concentrations

Constituent	Concentration (%w/w)
Water	>95
Glycoproteins	1-2
Free Protein	0.5-1
Salts/Minerals	1

Mucus forms the upper layer of the ALF. Mucus is a mixture of water and mucin glycoproteins (as well as lipids, proteoglycans and salts/minerals)[8]. Glycoproteins are extremely large (molecular mass >1MDa) polymer-like molecules (see Figure 2.3). In human pulmonary mucus, the primary mucins expressed are MUC5b and MUC5ac[9]. The central backbone of the mucin monomer is composed of several cysteine rich domains and repeating regions of heavy glycosylation (O- and N-linked oligosaccharides). These regions are negatively charged with sialic acids and sulfate groups. Disulfide rich domains are found at the terminal ends of the monomer, which bundle together to stabilize the un-glycosylated regions of the protein, and which can crosslink with other monomers (end-to-end) to form a larger mucus network[10].

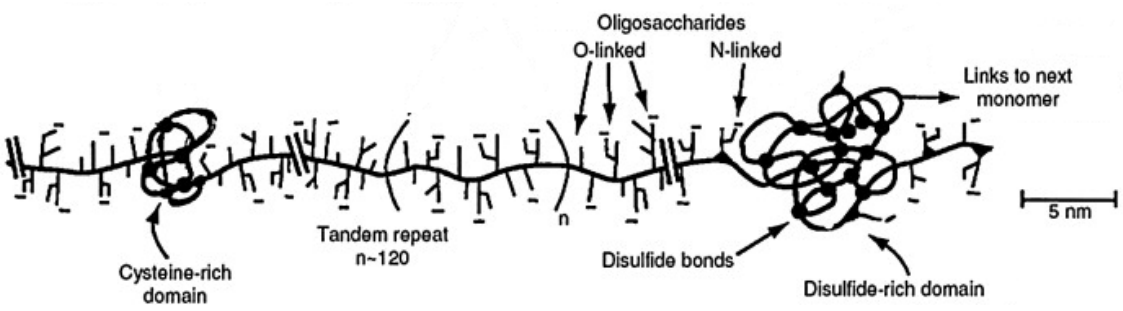

Figure 2.3: Mucin monomer structure[11]

Mucins are formed in goblet cells within the epithelial lining, and released into the sol sub-layer via a calcium-sodium exchange (Figure 2.4). They are initially tightly packed (due to high concentrations of calcium causing significant charge-shielding) but when released to the sub-layer, sodium ions exchange places with calcium ions, driving the folds and loops of the monomer to spread out and away from each other, rapidly expanding in size up to 600 fold.[12] These monomers interact with each other, forming non-covalent bonds, entangling or connecting through disulfide bridges. This results in an oligomeric mucin network from which the gel-like viscoelastic properties of mucus arises. This gel includes bound or "trapped" water, which associates with hydrophilic regions found along the mucin chains.[10]

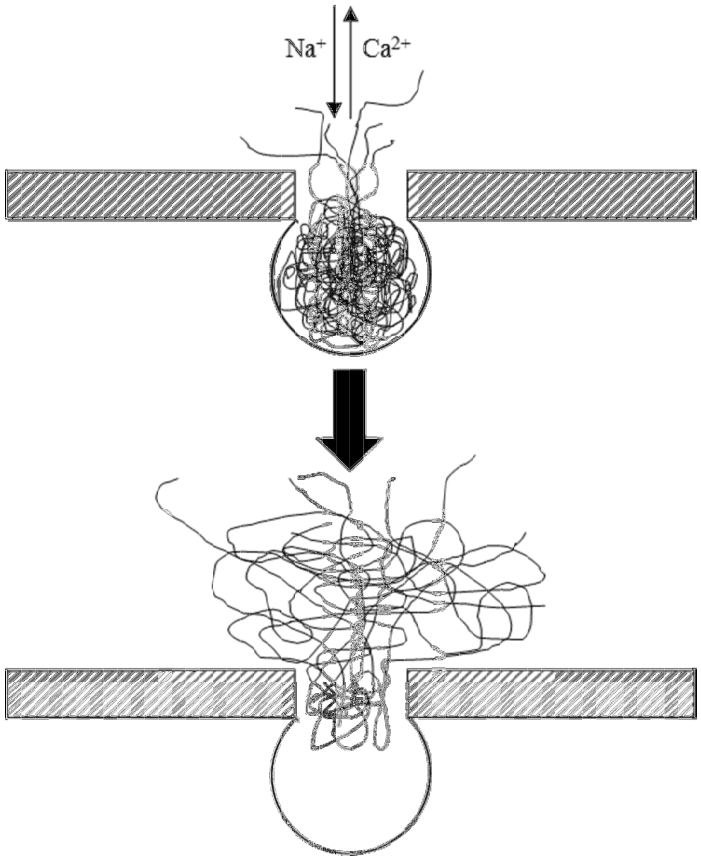

Figure 2.4: Mucin release from goblet cells, expansion via Ca-Na ion exchange[12]

The physical properties of the ALF are specifically adapted to achieve the protective coating which is its primary purpose. The viscoelastic nature of mucus provides an elastic and physical diffusion barrier to particle contaminants from the environment, while retaining a sufficiently viscous nature to allow transport and clearance, as well as maintaining a complete covering of the epithelial layer[10] (viscoelasticity will be discussed in greater detail within Chapter 4). In addition, pulmonary surfactant proteins, combined with lipids, reduce the work of breathing by preventing complete collapse and easier expansion of the alveolar termini of the pulmonary system. The surface tension is lowest in the alveoli, increasing throughout the lungs and towards the trachea[13]. Reported values for ALF physical properties vary widely as a result of methodology and conditions – ranges are listed in Table 2.2.

Table 2.2: Physical properties of the ALF

Property	Value
Viscoelasticity	
- Complex Modulus	5-50 Pa
- Loss Tangent	0.2-0.4
Surface Tension	
- Lower Airway	1-30 mN/m
- Upper Airway	30-60 mN/m
pH	6.8-7.2

The Pulmonary System:

The pulmonary system's purpose is to transport oxygen into the bloodstream while removing carbon dioxide. It is typically divided into two regions: the conducting portion, which is further separated into the upper airways (naso-pharynx, trachea and bronchi) and the lower airways (bronchioles and terminal bronchioles); and the respiratory portion, which includes the

respiratory bronchioles and alveoli (where the exchange of O_2 and CO_2 between air and blood occurs[14]).

The basic, simplified structure was introduced by E. R. Weibel[30] in 1963 and later adapted by Hinds[31]: beginning with the trachea, it consists of a series of bifurcated, roughly cylindrical elements in which the parent cylinder divides into two child cylinders of smaller diameter (the cross-sectional area of each child branch is decreased by a factor of 0.75[29]). This model treats each child-cylinder as equal, although in reality the need to make room for other internal organs means there is a difference in total volume between the right and left lobes of the lungs (which can result in differing sizes between child-cylinders). The angle between the two child cylinders is the bifurcation angle. Each bifurcation indicates the start of a new air-way generation, as indicated in Figure 2.5, beginning with the trachea numbered zero[14]. This system is employed so that each air-way generation is characterized by similar diameter and airflow velocities, despite differing locations in physical space.

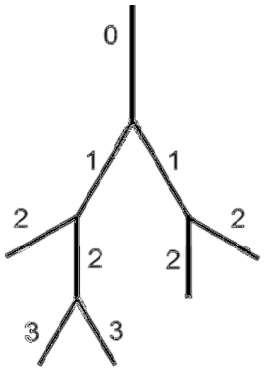

Figure 2.5: Airway generation numbering schematic[14]

Table 2.3 contains the average diameters and air velocities for different parts of the lungs. The airflow velocities for each subsequent generation are larger than half the value of the preceding generation due to the accompanying reduction in airway diameter. The overall result is a system which maximizes airflow while minimizing airflow resistance. This, in turn, reduces the amount of energy, or "work", required for breathing. Computation fluid dynamics (CFD) studies on tidal breathing within the lungs have confirmed this.[16]

Table 2.3: Dimensions and air velocities within the lungs[15]

Part	Number	Diameter (mm)	Length (mm)	Typical Air Velocity (m/s)
Nasal Airways		5-9		9
Mouth	1	20	70	3.2
Pharynx	1	30	30	1.4
Trachea	1	18	120	4.4
Two Main Bronchi	2	13	37	3.7
Lobar Bronchi	5	8	28	4
Segmental Bronchi	18	5	60	2.9
Bronchioles	504	2	20	0.6
Secondary Bronchioles	3024	1	15	0.4
Terminal Bronchioles	12100	0.7	5	0.2

Bioaerosol formation: Upper airway model

Bioaerosols form from the ALF, however the exact mechanism and origin within the pulmonary system remains controversial. Two basic mechanisms have been proposed, one taking place in the upper airways, the other in the lower. The former employs a shear-driven model to describe the process, in which surface-shearing of the ALF induces wave formation and propagation, potentially leading to instabilities and shedding of droplets[18] (see Figure 2.6). This process may occur whenever air is flowing across the ALF, although the likelihood of forming instabilities varies with surface tension, viscoelasticity and the applied shear force (resulting

from the air velocity at the interface). Hence, coughing and sneezing, in which much higher air velocities occur, are more likely to produce droplets (and in greater numbers) compared to tidal breathing.

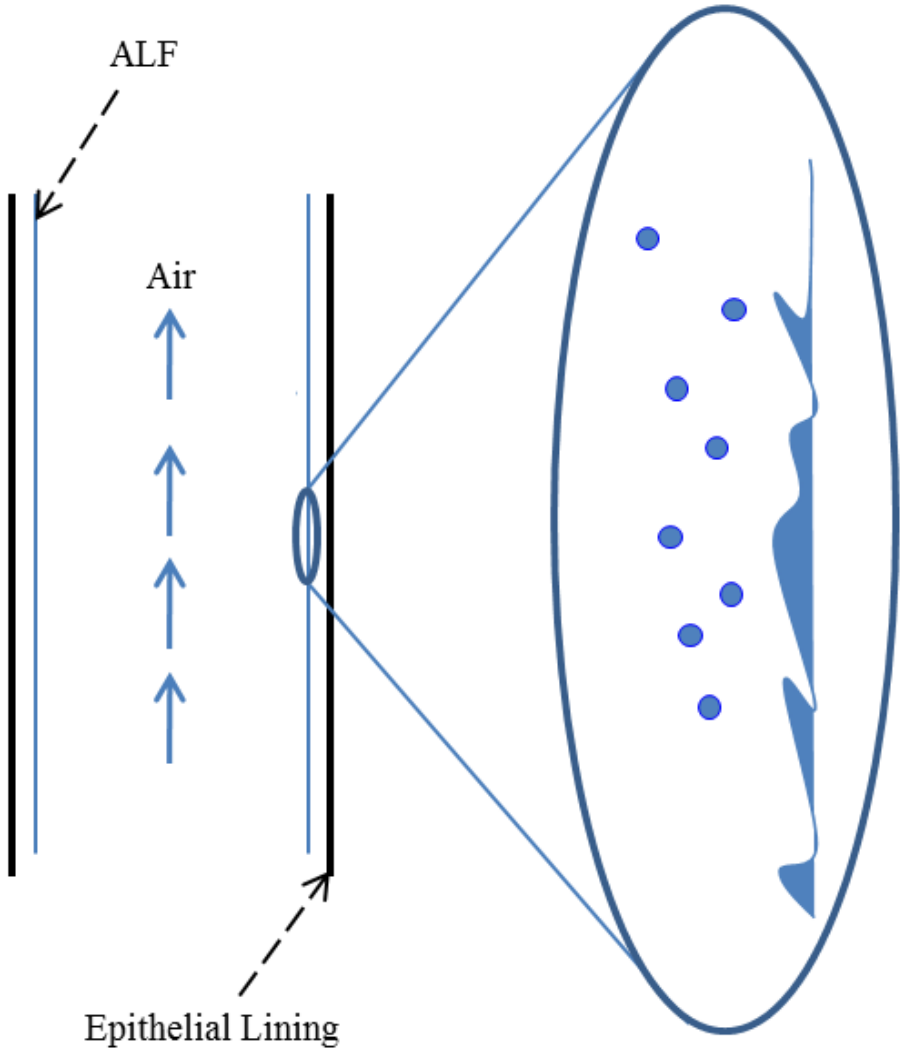

Figure 2.6: Droplet generation through shearing-induced wave formation

Furthermore, turbulence, characterized by chaotic and rapid variation in air flow patterns, can increase wave formation and drive the growth of instabilities. Reynolds Number (Re) is a

dimensionless parameter used to describe flow conditions. It is a ratio of the inertial to viscous forces acting on the fluid (equation I). Fully developed turbulent air flow is typically observed in fluid flows with Re greater than 4000, however transitory turbulence is observed for Re as low as 2000.

$$Re = \frac{\rho U D}{\mu} \qquad \text{(I)}$$

Where: ρ = Density of fluid (ρ_{Air}(37^{o}C) = 1.14 kg/m^{3})

U = Mean fluid velocity

D = Characteristic length/diameter of geometry

μ = Viscosity of fluid (μ_{Air}(37^{o}C) = 1.9E-5 kg/m*sec)

For body temperature (37^{o}C) tidal air flow through the trachea, Re is approximately 2100. This is near the lower threshold of the transitory flow regime, indicating both laminar and turbulent flows are possible. For cough air flow, which involves much higher velocities, Re is greater than 7000, so fully developed turbulent flow is expected. As a result, droplets are more readily formed during coughing compared to tidal breathing. In the lower airways, air flow velocities are significantly smaller than they are in the upper airways, and the Reynolds Number is of order unity or less, so minimal shearing is expected.

The shear-driven model has traditionally been considered an exhalation process, mostly due to describing cough and sneeze actions (which are expiratory); however, this may not be the case for tidal air flows. Experimental studies performed by Chowdhary et al. (1999, Journal of Asthma[32]) on physical models of the human trachea and bronchi, in which the wall shear stresses present for tidal air flow or cough air flow were measured, indicated peak wall shear stresses

were found along the inner wall just past the first and second bifurcation for tidal air flow. Coughing, on the other hand, is an expiratory process, with peak air flow rates as high as 12 L/sec, and during this process, interfacial shearing peaked within the trachea, as it is coupled to fully developed turbulent air flow. CFD models of the airways during tidal air flow (performed by A. Green in 2003[17] and Y. Wang et al. in 2009[33]) yielded similar results, and indicate that maximal surface shearing may occur during inhalation. These studies suggest that bioaerosol formation for tidal air flow may occur proximal to the first bifurcations and be an inhalation-stage process. If this is the case, then the bifurcation angle is expected to influence droplet formation. Furthermore, as an inhalation-stage process, there are ramifications in terms of auto-infection (the process of transmitting an infection deeper into the host's pulmonary system). This will be an important topic in the upcoming discussion of the lower airway model.

The experiments on air-shearing of mayonnaise in a rectangular channel performed by Basser et al. in 1989[34] serve as a guide to the relevance of physical properties on the formation of wave-instabilities. When mayonnaise – which is a stiff, non-Newtonian fluid – was placed on polyethylene, an oily sub-layer formed between the two. The critical air speed required to induce instabilities was reduced by half when the sub-layer was present, indicating the significance of having both viscous and elastic elements present. This importance was confirmed in the computational work performed by Moriarty and Grotberg,[18] in which an elastic solid upper layer was modeled with a Newtonian sub-layer beneath. Hence, the viscoelastic properties of the ALF are expected to be extremely relevant to bioaerosol formation.

Basser et al. excluded surface tension in their analysis, concluding that their system was analogous to wind-water waves in which gravity would dominate any surface tension effects.

This analogy does not translate well, as it assumes a deep fluid (in which the ratio of relevant wavelengths to depth is very small), whereas in the case of the ALF, the wavelengths must at least equal the size (diameter) of the droplets produced (less than 10 microns for bioaerosols), compared to a depth between 10-70 microns. This suggests the potential for surface tension effects to be relevant, and indeed, Moriarty and Grotberg found that adding a surface tension term to their model did significantly alter the results (compared to excluding it). However, once accounted for, reasonable changes in the value of the surface tension (from a physiological viewpoint) did not continue to significantly alter the outcome, particularly compared to changes resulting from the addition of a viscous sub-layer. Hence, changes in the surface tension in the upper airways are not expected to play a major role in bioaerosol formation.

Bioaerosol formation: Lower airway model

The second mechanism for bioaerosol generation, proposed by Johnson and Morawska, occurs in the lower airways, and involves droplets shedding from ruptured films (which form through the re-opening of collapsed bronchioles during tidal breathing[19]). The basic process occurs in four stages and is shown in Figure 2.7. In stage one the bronchiole has collapsed at the end of the previous expiratory phase. In stage two, inhalation has started and the bronchiole begins to open. ALF forms a bridge stretched across the bronchiole. In stage three, the bronchiole has completely opened, producing a bubble/film of ALF across the interior which subsequently breaks, generating droplets that are immediately entrained in the air stream. In stage four, the expiratory phase begins, the droplets are expelled, and the bronchiole begins to collapse again. The process is surface-tension dominated[20] – determining the capillary number (Ca, equation II), which is a dimensionless ratio of viscous forces to surface tension forces, yields a value of 0.2 (the zero-shear viscosity of mucus was used as an estimation of fluid

viscosity). Surfactant proteins in the ALF reduce surface tension (which is necessary to prevent alveolar collapse) – the reduced surface tension enables easy formation of thin films as the bronchioles open. The number of droplets produced is a function of the number of collapsed bronchioles and the frequency of their collapse. Some estimates of bronchiole collapse indicate that on average less than 10% of total bronchioles are prone to collapse[21], however exact amounts are currently unknown.

$$Ca = \frac{\mu U}{\gamma} \qquad \text{(II)}$$

Where: μ = Fluid viscosity (Estimated from zero-shear viscosity)

U = Velocity

γ = Surface tension

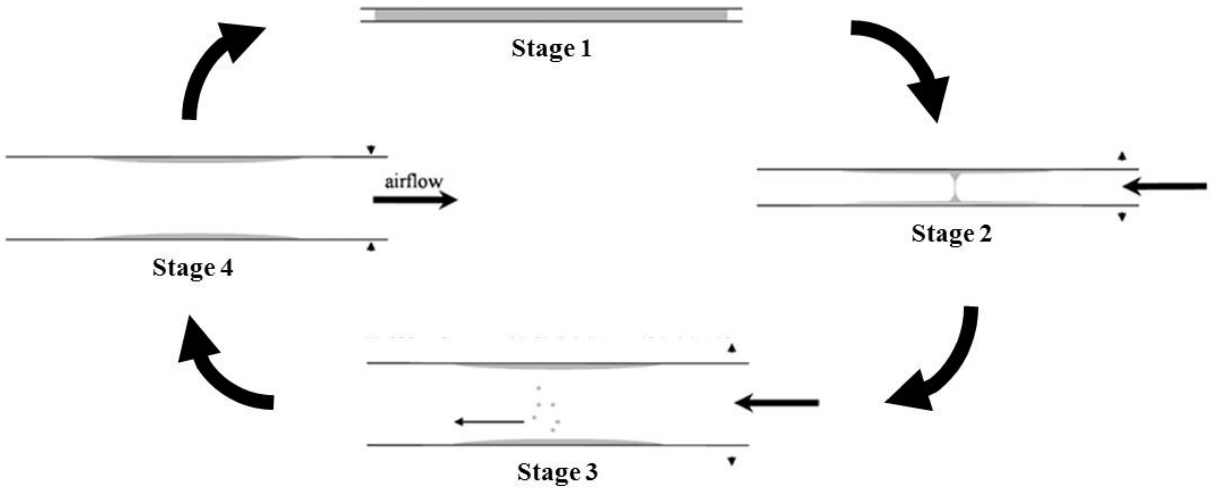

Figure 2.7: Stage-wise progression of droplet generation in lower airway (bronchioles)[19]

Support for this model is largely empirical, with several studies examining either expelled breath condensate or droplet number as a function of various breathing patterns. Johnson and Morawska, for their 2009 study, used an aerodynamic particle sizer to determine the droplet concentration and size expelled from 13 healthy volunteers. The subjects were directed to perform several different breathing maneuvers and the resulting droplet data was compared. They reported a decrease in droplet concentration (compared to normal breathing) when the subjects inhaled normally and then held their breath before exhaling, with the decrease tracking with the length of time the subjects held their breath. This suggests droplet formation occurs during inhalation, and that droplet settling occurs while breath is held. Furthermore, rapid tidal breathing generated more droplets only when inhalation speed was increased. This was taken as further evidence that bioaerosol formation during tidal breathing must be an inhalation process, and that the mechanism must be film-rupture; however this assumed that the shear-driven mechanism in the upper airway was an exhalation-only process (for tidal breathing). While true for coughing or sneezing, this is not likely to be the case for tidal air flows, as discussed previously. Thus, both mechanisms remain theoretically possible, and more evidence is needed to discard one or the other.

Droplet transport:

Droplets, no matter where they form in the lungs, will vary in size and their diameters will range from hundreds of nanometers to tens of microns. These droplets are immediately subject to a number of forces and processes, including transport and gravitational settling. Droplet evaporation is not expected to occur within the pulmonary system because it is a moist, humid environment (relative humidity approaching 100%). Outside the lungs, evaporation can occur and will depend on the specific environmental conditions. As evaporation occurs, droplet

diameter decreases, so that larger droplets can shrink to become aerosols. Critical particle diameter can be reached and will depend on the composition of the droplets, especially in regards to salt content. In terms of transportation, the two most likely methods are diffusion and advection (by the air stream). The Péclet number (Pe) is a dimensionless ratio of the rate of advection (due to bulk fluid flow) to the rate of diffusion (equation III). The larger the value for Pe, the more dominant advection is compared to diffusion, and vice versa for values smaller than one. A simple order of magnitude analysis of droplets within the pulmonary system leads to an estimate of Pe as follows:

$$Pe = \frac{lU}{D} \qquad \text{(III)}$$

Where: l = Transport length scale

U = Mean air velocity

D = Diffusivity

Diffusivity can be calculated as follows:

$$D = \frac{k_b T}{6\pi\mu d} \qquad \text{(IV)}$$

Where: k_b = Boltzmann's Constant

T = Temperature

μ = Viscosity of the bulk media

d = Droplet diameter

Diffusivity is inversely proportional to droplet size (larger droplets result in greater surface drag forces, reducing mobility), and will remain constant throughout the pulmonary system (for a given droplet size); therefore Pe should be proportional to droplet size. The length scales of interest are on the order of millimeters to centimeters (based on the diameter of the airways and the total length of the pulmonary system). The lowest mean air velocity occurs in the terminal airway generations – because Pe varies linearly with velocity, it will be minimized when velocity is at a minimum (for fixed diffusivity and length scale). Pe was calculated for a range of droplet sizes and length scales: the results are shown in Table 2.4. Advection is dominant for all conditions throughout the pulmonary system, which indicates that respiratory air flow rates are extremely relevant to droplet transport.

Table 2.4: Pe for a range of droplet sizes

Droplet Diameter (μm)	Length Scale (mm)			
	0.1	1	10	100
0.1	$O(10^5)$	$O(10^6)$	$O(10^7)$	$O(10^8)$
1	$O(10^6)$	$O(10^7)$	$O(10^8)$	$O(10^9)$
10	$O(10^7)$	$O(10^8)$	$O(10^9)$	$O(10^{10})$

Similarly, the gravitational settling rate can be determined as a function of droplet size. Figure 2.8 shows the forces acting on a spherical droplet in stagnant air. Using Stoke's law to determine the drag force acting on the droplet as a function of settling velocity (equation V), and equating that to the gravitational force acting on the particle as a function of droplet diameter (equation VI) the settling velocity can be determined as a function of droplet diameter (equation VII). Calculating the settling velocity for a range of droplet sizes (shown in Figure 2.9) indicates settling velocities become negligibly small for droplets with diameters less than 10 micron.

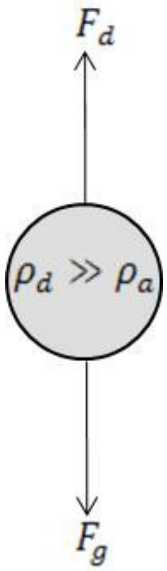

Figure 2.8: Schematic of forces acting on settling droplet

$$F_d = 3\pi\mu d u_s \qquad \text{(V)}$$

$$F_g = m_d g = \rho_d V_d g = \frac{1}{6}\pi\rho_d d^3 g \qquad \text{(VI)}$$

$$u_s = \frac{\rho_d g d^2}{18\mu} \qquad \text{(VII)}$$

Where: μ = Viscosity of the bulk media

d = Droplet diameter

u_s = Settling velocity

m_d = Droplet mass

g = Gravitational acceleration

ρ_d = Droplet density

V_d = Droplet volume

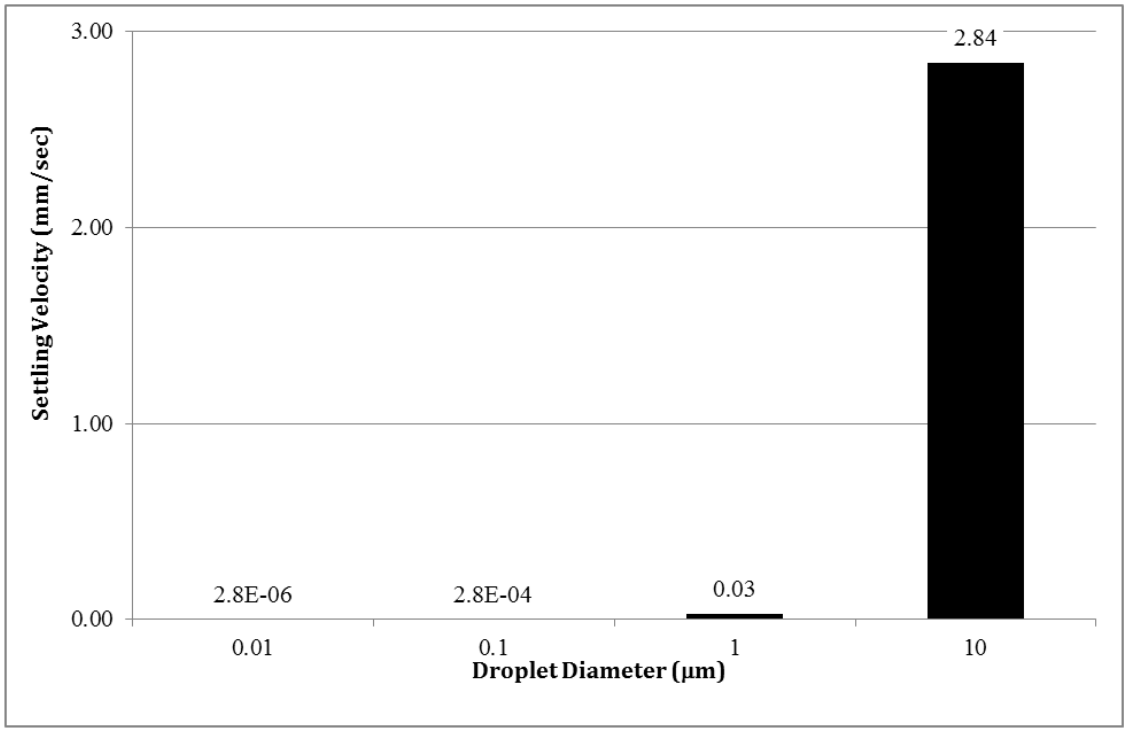

Figure 2.9: Settling velocity as a function of droplet diameter

Once formed, larger droplets (> 10 microns) will settle back to the ALF quickly, whereas smaller droplets will remain entrained within the air stream. In order for transmission to occur, however, the droplets must first escape the lungs. This occurs during the expiratory phase, which typically lasts from one to three seconds, so the droplets must be transported from their point of origin to the nasal airways or mouth and out to the environment within that period of time. A rough estimate of escape time can be determined from the length the droplets must travel through each airway generation and the mean air velocity within that generation. The total length droplets formed in the upper airways must travel to escape is between 0.22 meters and 0.29 meters. Traveling at the mean air velocity for each airway generation, they would require less than 0.1 seconds to traverse the total distance. Droplets formed in the lower airways must travel an additional 0.02 – 0.1 meters (for a total distance between 0.24 meters and 0.39 meters). The time

required for these droplets to escape is less than 0.6 seconds. Droplets are therefore theoretically capable of escaping the pulmonary system (from either point of origin) during the expiratory phase of tidal breathing. During a cough or sneeze much higher air velocities are achieved, therefore droplets are expected to escape to the environment in even less time compared to tidal breathing.

Conclusion:

Two primary mechanisms for droplet formation during tidal breathing were discussed: an upper airway and a lower airway model. Investigation of published experimental and computational data indicated the upper airway model may actually be an inhalation-process. If true, droplet formation is likely to be a function of bifurcation angle. Furthermore, published research thought to support the lower airway model would actually fit the new upper airway model as well, so that neither model can be confirmed or denied, therefore droplets may potentially form in either the upper or lower airways. These droplets are composed of ALF along with anything residing in or on the ALF, including pathogens. In this way, pathogens captured in these droplets are capable of escaping to the surrounding environment. Upon reaching the environment, large droplets will settle or evaporate, decreasing their size until they reach a critical equilibrium diameter (which is a function of their composition). At these small sizes (a few nanometers to a few microns in diameter) the rate at which they settle, due to gravity, is virtually insignificant. Instead, they will remain airborne – transported along air currents where they may eventually be inhaled by other individuals, and result in an infection.

References:

1. Wathes, C. M.; Cox, C. B. (1995). *Bioaerosols handbook*.
2. Williams, R.; Rankin, N; Smith, T; Galler, D; Seakins, P (1996) *Crit Care Med* 24: 1920-1929
3. Knowles, M. R.; Boucher, R. C. (2002) *J Clin Invest.* 109(5): 571–577
4. http://www.lungusa.org/asthmasteroids
5. Mescher, A. L. (2010) *Junqueira's Basic Histology: Text and Atlas, 12e*, Ch. 17
6. Delmotte, P.; Sanderson, M. J. (2006) *Am. J. Respir. Cell Mol. Biol.* 10: 1165
7. Jeffery, P. K.; Reid, L. M. (1977). *The respiratory mucus membrane. Respiratory defense mechanisms. Part I*: 193–245.
8. Takishima, T.; Shimura, S. (1994) *Airway Secretion: Physiological bases for the control of mucous hypersecretion*, Ch. 6: 224-225
9. Takishima, T.; Shimura, S. (1994) *Airway Secretion: Physiological bases for the control of mucous hypersecretion*, Ch. 2
10. Lai, S. K.; Wang, Y.; Wirtz, D.; Hanes, J. (2009) *Advanced Drug Delivery Reviews* 61(2): 86-100
11. Ogra, P. L.; Mestecky, J.; Lamm, M. E.; Strober, W.; Bienenstock, J.; McGhee, J. R. (1999) *Mucosal Immunology*: 43-64
12. Rogers, D. F.; Lethem, M. I. (1997) *Airway Mucus: Basic Mechanisms and Clinical Perspectives*, Ch. 6: 119-122
13. Notter, R. H. (2000) *Lung Surfactants*, Ch. 6
14. Thurlbeck, W. M.; Churg, A. M. (1995) *Pathology of the lung, 2e*, Ch. 3: 90-94
15. Zeng, X. M.; Martin, G.; Marriott, C. (2001) *Particulate Interactions in Dry Powder Formulations of Inhalation*
16. Mihaescu, M.; Murugappan, S.; Gutmark, E.; Donnelly, L. F.; Khosla, S.; Kalra, M. (2008) *Ann Otol Rhinol Laryngol* 117(4): 303-309
17. Green, A. S. (2004) *Journal of Biomechanics* 37(5): 661-667
18. Moriarty, J. A.; Grotberg, J. B. (1999) *J. Fluid Mech.* 387: 1-22
19. Johnson, G.; Morawska, L. (2009) *J Aerosol Med Pulm Drug Deliv*. 22:1-9.
20. Hazel, A. L.; Heil, M. (2005) *Proc R. Soc.* 461: 1847-1868
21. Macklem, P. T.; Proctor, D. F.; Hogg, J. C. (1970) *Respir Phsysiol.*8:191–203
22. Israelachvili, J. (1991) *Intermolecular and Surface Forces*
23. Johnson GR and Morawska L: The mechanism of breath aerosol formation. J Aerosol Med Pulm Drug Deliv. 2009;22:1-9.
24. Gebhart, J.; Anselm, J.; Heyder, J.; Stahlhofen, W. (1988) *J. Aerosol Med.* 1: 196-197
25. Morawska L, Johnson GR, Ristovski ZD, Hargreaves M, Mengersen K, Corbett S, Chao CYH, Li Y, and Katoshevski D: Size distribution and sites of origin of droplets expelled from the human respiratory tract during expiratory activities. J Aerosol Sci. 2009;40:256-269
26. Kataoka, I.; Ishii, M.; Mishima, K. (1982) *J. Fluids Eng.* 105: 230-238
27. Blanchard, D. (1963) *Progr. Oceanogr.* 1: 73-202
28. Engel, L.; Grassino, A.; Anthonisen, N. (1975) *J. Appl. Physiol*. 38:1117-1125
29. Haskin, P.; Goodman, L. (1982) *AJR* 139: 879-882
30. Weibel, E. (1963) *Morphometry of the human lung*
31. Hinds, W. (1982) *Aerosol technology: properties, behavior and measurements of airborne particles*
32. Chowdhary, R.; Singh, V.; Tattersfield, A.; Sharma, S.; Subir, K.; Gupta, A. (1999) Journal of Asthma 36(5): 419-426
33. Wang, Y.; Liu, Y.; Sun, X.; Yu, S.; Gao, F. (2009) *Acta Mech Sin* 25: 737-746
34. Basser, P.; McMahon, T.; Griffith, P. (1989) *J. Biomech. Eng.* 111: 288-297

Chapter 3: Bioaerosol generation – *in vitro* models

Introduction:

The first hypothesis of this thesis is:

> Droplet generation during tidal breathing can occur in both the upper airways (via surface shear) and lower airways (via film rupture) during inhalation, and will vary with bifurcation angle in the upper airways.

To address this hypothesis, novel *in vitro* models were developed which were designed to replicate the conditions within the pulmonary system that occur during droplet formation (via the two potential mechanisms proposed in the literature). A cough model was developed as well and is expected to produce the largest number of droplets (via shearing) due to the much higher air velocities present. Experiments were performed with each system to examine droplet production in terms of number and size.

Background:

In chapter 2, bioaerosol transport through the pulmonary system was shown to be technically feasible. Two major mechanisms for droplet generation during tidal breathing were identified from the literature: films or plugs of ALF rupturing in the lower airways (Johnson and Morawska, 2009[18]); and surface shearing of ALF in the upper airways (Moriarty and Grotberg, 1999[17]). While the role of surface shearing in droplets generated via coughing or sneezing is widely accepted, for tidal breathing air flow rates recent studies[18-20] of exhaled droplets as a function of breathing pattern have reported circumstantial evidence favoring droplet formation as an inhalation process. This was taken to mean that the lower airway is the more probable source of exhaled droplets; however, evidence was presented in chapter 2 suggesting that wall shear stress in the upper airways may peak during inhalation subsequent to bifurcations in the first few

generations of the airways, indicating the possibility that the shear-driven mechanism for droplet generation may also be an inhalation process (and therefore in agreement with the expelled droplet data). If this is the case, then the bifurcation angle is expected to influence droplet formation in the upper airway model (due to shifting the peak air velocity closer to the inner wall, thereby increasing wall shear stress), and forms the basis for the first hypothesis of this thesis.

Optical Particle Counting Systems:

To test the mechanisms for bioaerosol generation discussed in chapter 2, the first requirement is a means to determine when droplets are present and in what numbers (as well as both their size and size distribution). As discussed previously, the presence of small droplets was expected even in the 1940s (Duguid[21]) but thought to be insignificant, mostly due to the inability to observe them. This persisted until the 1990s, after the development of optical particle counters (OPCs), which were employed by Papineni and Rosenthal[22] to measure expelled droplets. They found that the number of small droplets vastly exceeded the number of larger droplets and paved the way for a deeper understanding of airborne transmission.

OPCs come in many shapes and sizes, but the basic mechanism involves measuring laser light that has been blocked or scattered by particles passing through the beam[1]. Refraction and diffraction are used to measure the size and number of particles (Figure 3.1). To produce accurate, repeatable results, they operate at fixed air flow rates as a closed system. Limitations of this method involve the optical particle concentration: if the number of particles per volume of air is too great, secondary and tertiary scattering can skew the results (or the intensity may become too low); too few particles per volume and insufficient scattering may occur.

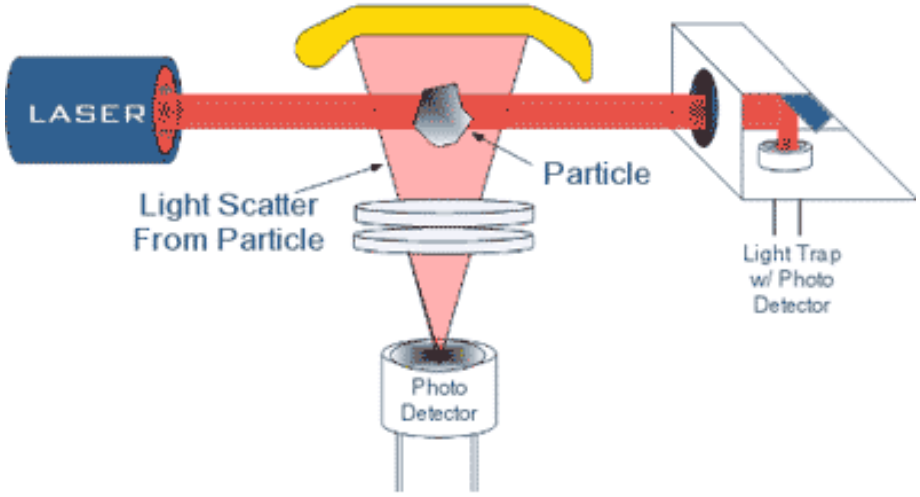

Figure 3.1: Optical particle detector array[2]

Many commercially available OPCs used for medical and device research operate at flow rates equivalent to peak respiratory rates (such as 1 CFM or 28.3 sLPM). When activated, they measure continuously in real-time (sampling times are typically in the 1-3 millisecond range).Vacuum pumps are used to maintain air flow at the specified flow rate (and are often controlled by software which constantly monitors and adjusts for pressure drops which may occur upstream during sampling). These OPCs work well provided they can sample from continuously supplied air. As a consequence, they are well-suited for use in systems operating at tidal breathing flow rates, but require a more sophisticated setup to work with cough-air systems (in which air flow rate varies rapidly and achieves a peak value many times that of tidal breathing). To that end, the Exhalair bioaerosol measurement system (pictured in Figure 3.2) was created by Pulmatrix, Inc (Lexington, MA). The system uses an Airnet optical particle counter (from Particle Measuring Systems, Boulder, CO) coupled to a vacuum pump along with a flow

meter and is specifically designed to measure droplets in exhaled tidal- and cough-air while simultaneously measuring the air flow rate.

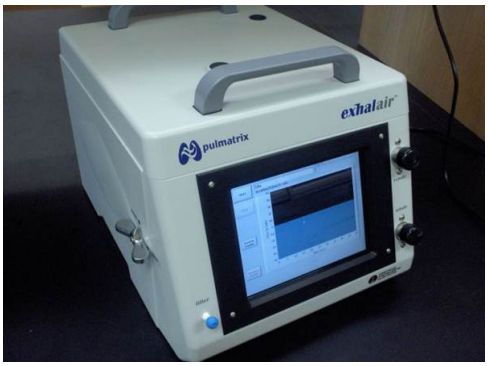

Figure 3.2: Exhalair system for measuring droplets in exhaled air (Pulmatrix, Inc.)

Exhaled air is sampled at 28.3 sLPM – if supply air flow rate is greater than the sampling rate, excess air is diverted through one-way valves and exhausted through an ultra-low penetration air (ULPA) filter (designed to remove greater than 99% of particles greater than 120 nm in size); if less, the sample air is mixed with ULPA filtered, “clean” air at a known ratio. This is advantageous in that it enables accurate droplet measurement for a variety of breathing patterns (i.e. tidal breathing at varying rates/volumes, cough-air flows, etc.), however it does require the assumption that droplets within the exhaled air are well-mixed, so that sampling a portion of said air remains an accurate assessment of overall droplet number.

Lower Airway Model Development:

As described in Chapter 2, the lower airway mechanism of droplet generation involves the reopening of collapsed bronchioles, producing a thin film that subsequently breaks into fine particles. The droplets are created only during the re-opening stage (as the bronchiole expands),

therefore mimicking this step is the minimum requirement of a bench-top system. This was accomplished utilizing conical tubes with a maximum diameter equal to that of the fully dilated bronchioles and a minimum diameter selected such that a liquid meniscus or film can be created by careful sample loading. The minimum diameter was also used as an orifice to control the air flow rate through each tube. Figure 3.3 is a schematic diagram of this system: multiple tubes are used to prevent the need for additional clean air when measuring with the OPC (the system was designed to operate at 28.3 sLPM), which would dilute the sample air stream. A total of 96 tubes were used in a parallel flow configuration, to maintain an equal pressure drop across each tube.

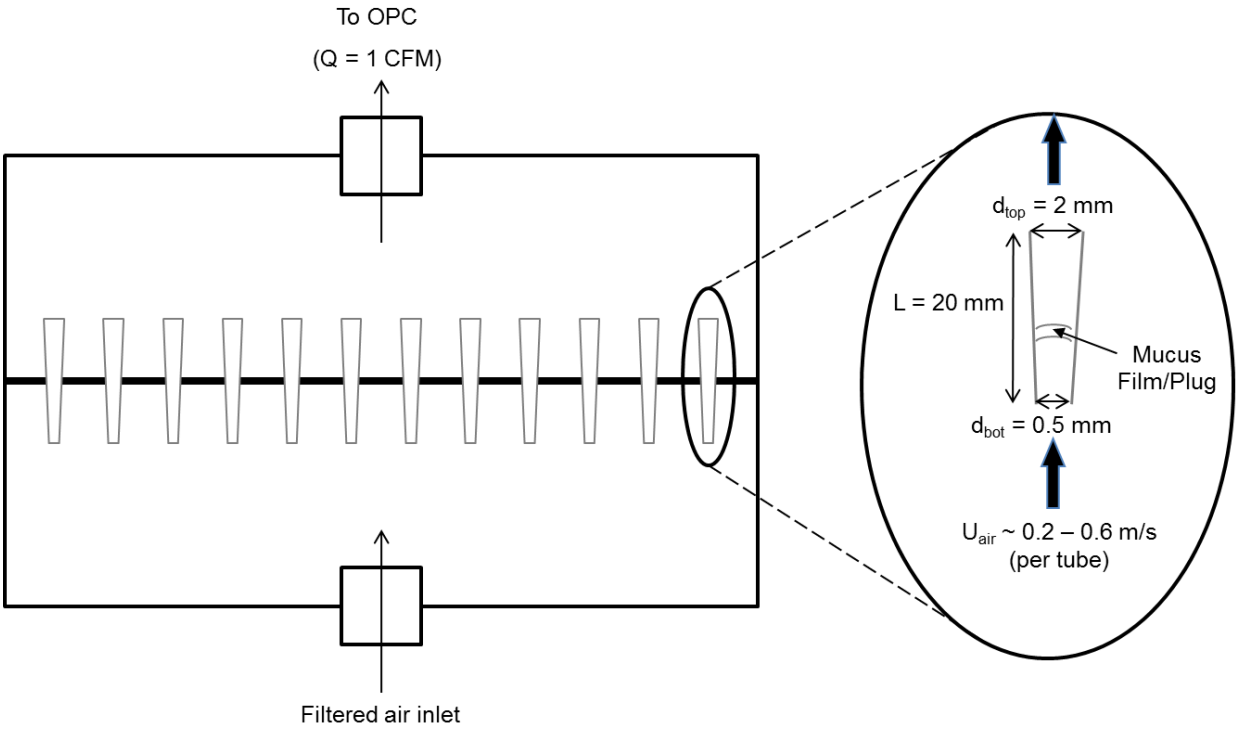

Figure 3.3: Schematic diagram of lower airway droplet system

One-way valves were employed at the entrance and exit of the otherwise closed system containing the simulated bronchiole tubes to prevent air flow in the reverse direction. The tubes

were spaced about three tube-lengths (60 mm) from the entrance and exit, to reduce center-to-edge variations in pressure drop and air flow. The tubes are the only passage between the upper and lower halves of the chamber, which were otherwise completely sealed from each other. Sample loading was accomplished via pipette, with care taken to ensure a film/plug was formed in each tube prior to starting the experiment. Capillary forces were sufficient to prevent the sample from draining (by gravity) from the lower end of each tube.

During operation, a vacuum pump (from the OPC) creates a pressure drop across the entire system to achieve an overall air flow rate of 28.3 sLPM. Air is drawn into the lower chamber through an ULPA filtration system to prevent contamination from the environment, then passes through the tubes and ultimately into the OPC. Each tube experiences an equivalent pressure drop due to their parallel configuration and spacing from the container walls. Along with air, the sample film is driven upwards through the tube. Due to the conical shape of the tube, the film expands as it moves, mimicking the film expansion that occurs within the expanding bronchioles *in vivo*, until it reaches a critical thickness/area and breaks, shedding droplets which are entrained within the air stream and drawn out to the OPC.

Upper Airway Model Development:

The upper airway model describes a shear-driven mechanism for droplet generation. Shear stresses along the ALF are proportional to the velocity of the air passing over it, so shear stress is expected to be highest in the upper airways and trachea, where the velocity peaks. Early *in vitro* systems to study cough-generated shear forces on the ALF were created by King et al. in the 1980s with the initial motivation to study how shearing from air flow was involved in mucus transport and clearance[3,4]. These studies used a simulated cough system consisting of a

rectangular channel in which mucus or mucus simulants were placed as a thin layer coating the bottom of the channel. The dimensions of the channel were such that the cross-sectional area (but not shape) was similar to that of the human trachea. Air was forced through the channel by generating a high pressure bolus of air upstream to produce flow rates matching those in the trachea of humans during coughing. A schematic of this system is shown in Figure 3.4

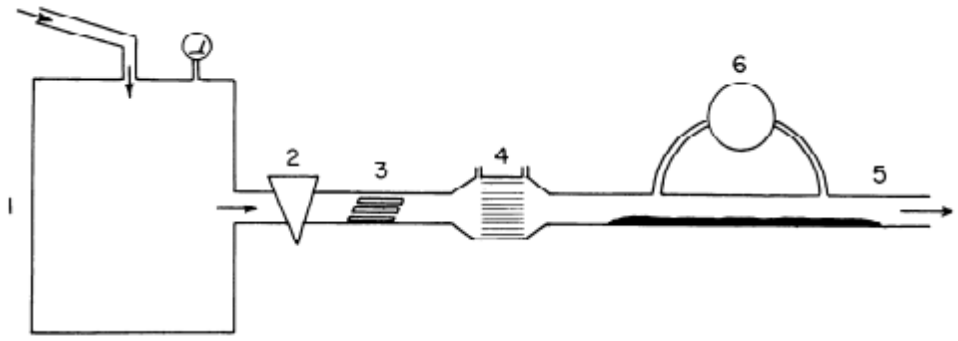

Figure 3.4: Schematic of King's simulated cough system – (1) Air tank;(2) Solenoid valve; (3) Laminar flow element;(4) Pneuomotachograph;(5) Trough (model trachea);(6) Differential pressure transducer[7]

This model was adapted for use in studying droplet generation from cough shearing by Edwards and Watanabe et al.[6,7] by adding a collection vessel on the outlet and sampling with an OPC. An ULPA filter was also added prior to the trough to prevent particle contamination from upstream components. The collection vessel was basically a chamber-and-piston setup with variable volume. This acted to contain the cough-air exhaled from the trough, but meant that the air remained stagnant for several minutes while the OPC sampled the entire cough volume at a fixed volumetric flow rate (28.3 sLPM). Droplet deposition along the walls of the container over the duration of time spent sampling the exhaled air could potentially result in lower measurements of total droplets produced. Furthermore, the square cross-section of the trough and the use of laminar flow elements altered the air-flow profile experienced by the mucus, and could

significantly influence droplet production, potentially resulting in a poor "fit" to the real pulmonary system. To compensate for these factors, the system was overhauled to create a new and improved simulated cough system.

Simulated Cough System:

The collection vessel was eliminated in the new simulated cough system – it was replaced by real-time sampling via an Exhalair. The air tank at the inlet of the system was replaced by a Breathing Simulator (MH Custom Design and Mfg., Midvale, UT), which is capable of generating specific, repeatable air-flow profiles. The simulated cough profile fed to the Breathing Simulator was generated from a mathematical model developed by Chen et al.[8] to fit data collected from volunteers. The final flow profile used is shown in Figure 3.5, with a peak flow rate of 6 liters per second (360 sLPM), a total duration of just under 0.4 seconds and a total volume of approximately 1 liter. Cough air exiting the trough was sampled by the Exhalair system at 28.3 sLPM, with excess air exhausting to an ULPA filter.

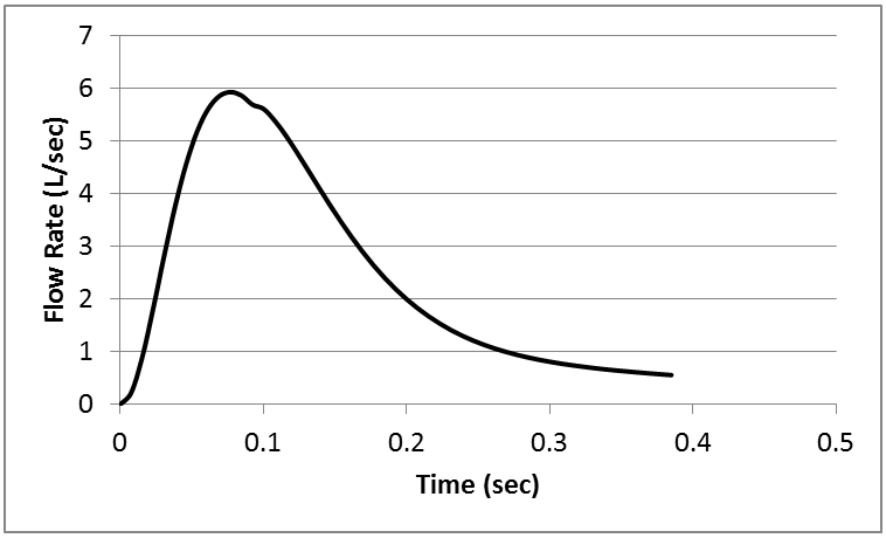

Figure 3.5: Cough-air flow profile

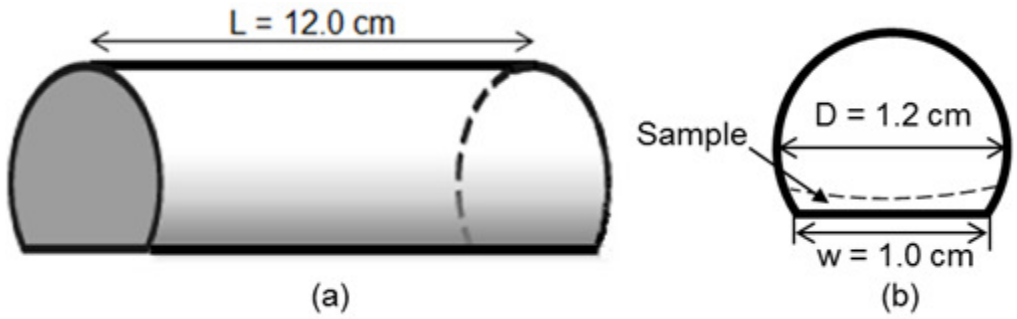

Figure 3.6: (a) Modified cough-trough (b) Cross-sectional schematic of modified cough-trough

The rectangular-channel trough was replaced with a nearly-cylindrical geometry (with a flattened section, see Figure 3.6). The primarily cylindrical geometry was used to reduce artifacts in air flow caused by the corners of the rectangular channel (compared to within the pulmonary system). The diameter of the cylindrical portion is equal to that of the trachea during a cough, which is smaller than for tidal breathing because the trachea constricts immediately prior to coughing (to further increase air velocities and thereby increase shear forces and clearance[9]). The flattened portion was incorporated to maintain a more uniform height of the mucus sample, which is spread over a fixed area at fixed volume. The exposed sample area is approximately 10 cm^2 or about 20% of the surface area of the human trachea. The final system is shown in Figure 3.7.

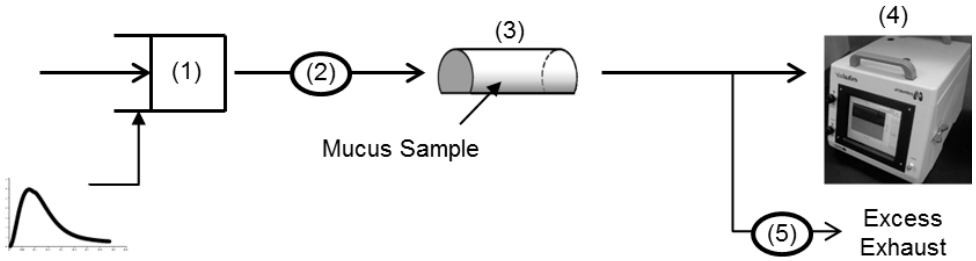

Figure 3.7: Simulated Cough System - (1) Breathing simulator; (2) ULPA filter; (3) Modified trough; (4) Exhalair; (5) Exhaust ULPA filter

Tidal breathing system:

The simulated cough system was also used to explore droplet formation during tidal breathing, although the following adjustments were required: the diameter of the model trachea was increased to 1.8 cm and the air flow profile fed to the breathing simulator was changed to a simple step-function with a maximum air flow rate of 28.3 sLPM (to simulate normal exhalation). However, in order to investigate whether the bifurcation angle influences droplet generation during inhalation, a separate system was developed. A physical model was created with physiologically appropriate dimensions and adjustable bifurcation angle, as shown in Figure 3.8. One arm of the bifurcation contained the sample on a horizontal plane located where surface shear forces were expected to reach a maximum, as indicated by CFD studies of the upper airways performed by Green (2004)[10] and Wang et al. (2009)[23]. Both arms were connected to an OPC with vacuum-pump controlled air flow rate.

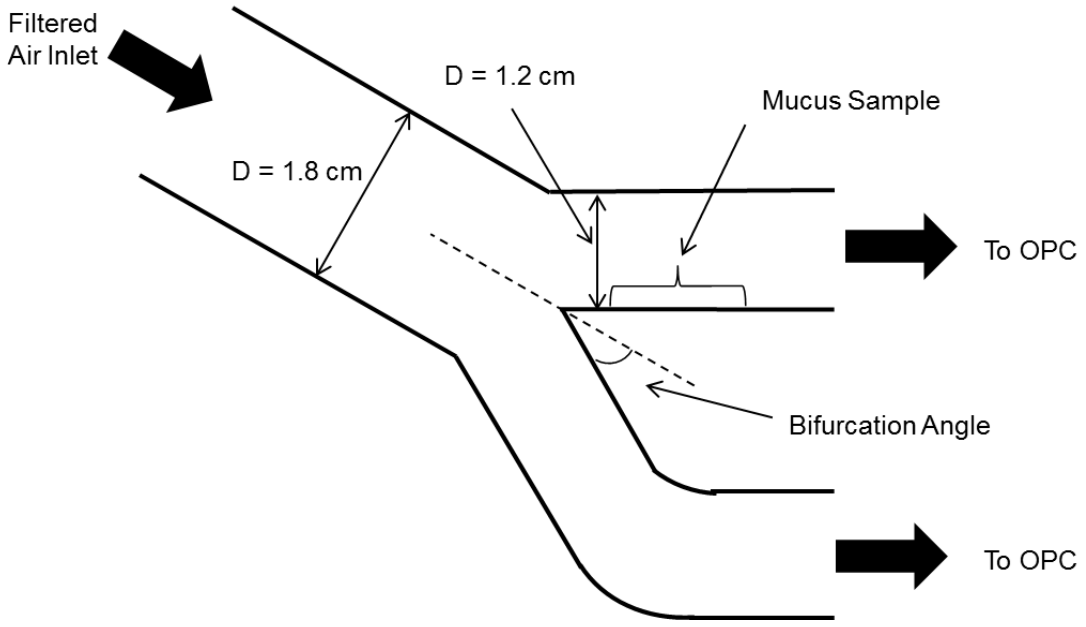

Figure 3.8: Tidal breathing system with adjustable bifurcation angle

Sample Mucus:

Healthy ALF is only present in small volumes and is extremely difficult to collect. A frequently used substitute is simulated epithelial lining fluid (sELF). sELF is a prepared solution of commercially available pig gastric mucin (1.5%w/w PGM, Sigma) and dipalmitoylphosphatidylcholine (1%w/w DPPC, Sigma) in Hank's balanced salt solution (HBSS, Sigma). DPPC is the lipid found in lung surfactant which is primarily responsible for reducing surface tension[11]. Reconstituting DPPC in solution was accomplished according to the procedure outlined by Pinazo et al.[12] The physical properties of sELF are shown in Table 3.1 – viscoelastic parameters were measured with an AR-G2 rheometer (TA Instruments, New Castle, DE); surface tension was measured with a SITA t60 bubble-pressure tensiometer (SITA Messtechnik, Dresden, Germany). All samples were loaded into the system in a particle free environment to avoid background contamination.

Table 3.1: sELF physical properties

Property	Value
Viscoelasticity	
- Complex Modulus	5 Pa
- Loss Tangent	0.38
Surface Tension (0.2 Hz)	31 mN/m
pH	7

Results:

Results for each system are presented as droplet concentration (the total number of droplets per liter of sample air – and per tube/bronchiole for the lower airway model) and are shown in Figure 3.9. Coughing produced the largest concentration of droplets (122 per liter of air +/- 20), as expected. Reported measurements of droplets produced by cough from healthy volunteers vary, ranging from several hundred to a few thousand per liter[13,14]; however this includes contributions from the mouth and pharynx. Furthermore, the exposed sample interfacial area in the simulated cough system is approximately 20% of that in the human trachea. On a per area basis, the simulated cough system produced 12.2 droplets per liter per square centimeter, compared to approximately 15.4 per liter per square centimeter for healthy human volunteers,[13] which is reasonably good agreement.

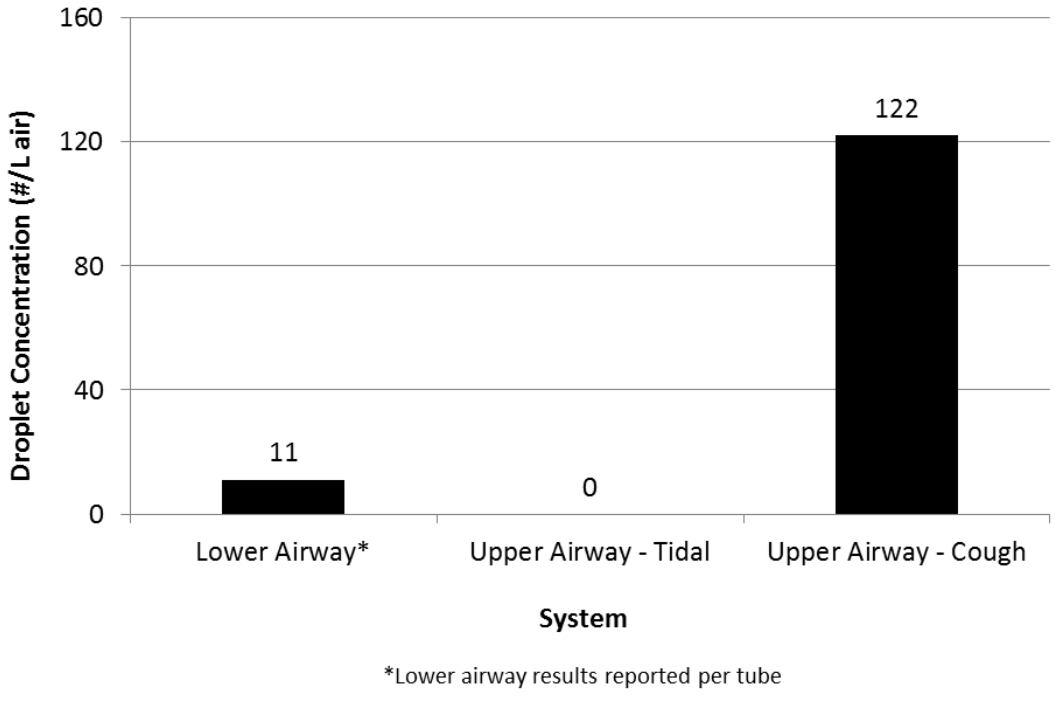

Figure 3.9: Cumulative droplets per liter of air produced by each system

The lower airway system produced an average of 11 +/- 3 droplets per liter of air per tube. Reported droplet numbers produced via tidal breathing by healthy volunteers varies widely within the literature, with concentrations ranging between 1 and several thousand, even between different individuals.[6,13,14] This makes a direct comparison difficult, however Edwards et al. (PNAS, 2004)[6] found that between 20% and 30% of the subjects in their study if expelled droplets produced significantly more droplets than the rest of the study group. They defined this group as "super-producers" (characterized as producing greater than 500 droplets per liter air). Using this cut-off as a guide, a minimum of 46 bronchioles simultaneously collapsing and expanding would be needed to reach the threshold of super-producing. This represents approximately 10% of the total number of bronchioles in healthy adults.

Adapting the simulated cough system for tidal breathing resulted in zero droplets. This was consistent with the results from the bifurcation system as an approximation for a zero degree bifurcation angle. The bifurcation system results are shown in Figure 3.10 (adjusted to a per exposed surface area basis) – droplet concentrations decreased as bifurcation angle decreased and vice versa. For adults, the average bifurcation angle of the bronchi (as measured by radiographs) is 30 +/- 6 degrees.[15] Bioaerosol concentrations increased significantly for bifurcation angles between 35 and 40 degrees, and approached the threshold for super-producing (~18 droplets per liter per square centimeter) around 38 degrees. This suggests that critical air velocity at the ALF interface is achieved for a bifurcation angle between 35 and 40 degrees. Based on these results, a small portion of the population, much less than 20%, is expected to fall into the super-producer category based on bifurcation angle alone.

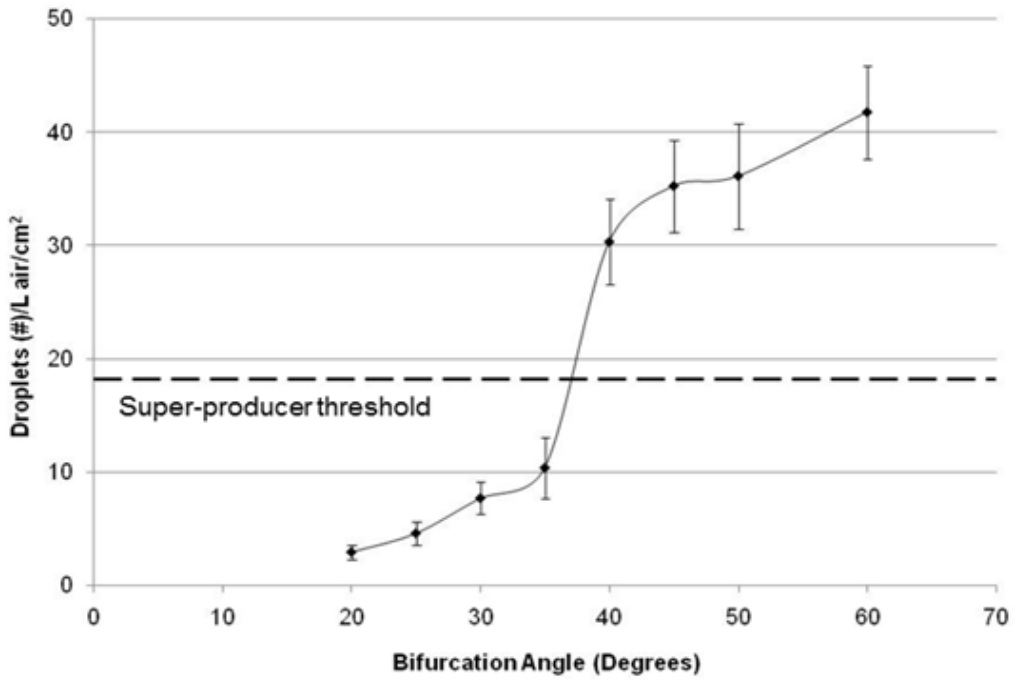

Figure 3.10: Bifurcation system results: Droplets per liter air per square centimeter exposed ALF

Conclusion:

In vitro systems were developed to replicate conditions for bioaerosol formation and measure the number of droplets formed according to the mechanisms discussed in chapter 2: a lower airway system designed to mimic bronchiole expansion and film rupturing; a shear-driven trachea model for both tidal and cough air flow patterns; and a shear-driven model of the first bifurcation with variable bifurcation angle. The shear-driven cough model produced the highest concentration of droplets, as expected, and was in reasonable agreement with data reported in the literature.

Droplet formation was shown to depend on bifurcation angle for the shear driven model at tidal air flow rates, with no droplets measured from the trachea model. This supports the first

hypothesis, which states that bioaerosol generation in the upper airways for tidal airflows occurs during inhalation. This is actually consistent with the expelled droplet data produced by Johnson and Morawska (2009)[18] and Almstrand et al. (2010)[19] which indicated that droplets were more likely to be produced during inhalation (they concluded this meant the lower airway model was therefore the real mechanism however these findings suggest that is not the only possibility). This has ramifications for auto-infection as well: bioaerosol formation occurring in the upper airways during inhalation can yield droplet deposition deeper in the lungs (especially for larger droplets, greater than 10 microns in diameter). This can potentially move an existing or developing infection deeper within the pulmonary system.

While both tidal air flow systems examined were capable of producing sufficient droplets to meet the threshold for super-producing, the conditions under which either case was observed is unlikely to occur by itself in enough of the population to adequately explain the results reported by Edwards et al[6]. For instance, the results from the bifurcation system indicate that the angle required to surpass the droplet concentration threshold for super-producing was 45 degrees, which is greater than two standard deviations above the mean bifurcation angle. However, if the results from both the lower airway system and the upper airway system are taken together, a number of combined solutions become plausible. Super-producers may have some combination of both airway geometry (e.g. large bifurcation angle at the bronchi) and collapsing bronchioles which results in their large bioaerosol numbers. Alternatively, it may be that some super-producers are due to being outliers in terms of bifurcation angle, while others are due to having a large number of collapsing bronchioles. The combined total from all of these possibilities may then match the percentage of the population observed in Edwards' study.

References:

1. Jaenicke, R. (1971) *J. Aerosol Sci.*3(2): 95-111
2. http://www.particlecounters.org/
3. King, M.;Brock, G.; Lundell, C. (1985) *J. Appl. Physiol.* 58: 1776-1782
4. Chang, H.; Weber, M.; King, M. (1988) *J. Appl. Physiol.* 65(3): 1203-9
5. Soland, V.; Brock, G.; King, M. (1987) *J. Appl. Physiol.* 63(2): 707-712
6. Edwards, D.; Man, J.; Brand, P.; Katsra, J.; Sommerer, K.; Stone, H.; Nardell, E.; Scheuch, G.; (2004) *Proc. Natl. Acad. Sci.* 101(50): 17383-17388
7. Watanabe, W.; Thomas, M.; Clarke, R.; Klibanov, A.; Langer, R.; Katstra, J.; Fuller, G.; Griel, L.; Fiegel, J.; Edwards, D. (2007) *J. Colloid Interface. Sci.* 307(1): 71-78
8. Gupta, J.; Lin, C.; Chen, Q. (2009) *Indoor Air* 19: 517-525
9. McCool, F. (2006) Chest 129(1): 485-535
10. Green, A. S. (2004) *Journal of Biomechanics* 37(5): 661-667
11. Notter, R. (2000) *Lung Surfactants* Ch. 6: 129-149, Ch. 8: 171-203
12. Pinazo, A.; Wen, X.; Liao, Y.; Prosser, A.; Franses, E. (2002) *Langmuir* 18: 8888-8896
13. Fabian, P.; Brain, J.; Houseman, E.; Milton, D. (2011) *J Aerosol Med Pulm Drug Deliv*. 24(3):137-47
14. Morawska, L.; Johnson, G.; Ristovski, Z.; Hargreaves, M.; Mengersen, K.; Corbett, S.; Chao, C.; Li, Y.; Katoshevski, D. (2009) *Aerosol Sci*. 40: 256–269
15. Haskin, P.; Goodman, L. (1982) *AJR* 139: 879-882
16. Hsu, S.; Strohl, K.; Jamieson, A. (1994) *J Appl. Physiol.* 76(6): 2481-2489
17. Moriarty, J. A.; Grotberg, J. B. (1999) *J. Fluid Mech.* 387: 1-22
18. Johnson, G.; Morawska, L. (2009) *J Aerosol Med Pulm Drug Deliv*. 22:1-9.
19. Almstrand, A.; Bake, B.; Ljungstrom, E.; Larsson, P.; Bredberg, A.; Mirgorodskaya, E.; Olin, A. (2010) *J Appl Physiol.*108:584-588
20. Haslbeck, K.; Schwarz, K.; Hohlfeld, J.; Seume, J.; Koch, W. (2010) *J Aerosol Sci.* 41:429-438
21. Duguid, J. (1946) *British Medical Journal* 265-268
22. Papineni, R.; Rosenthal, J. (1997) *J Aerosol Med.* 10(2):105-116
23. Wang, Y.; Liu, Y.; Sun, X.; Yu, S.; Gao, F. (2009) *Acta Mech Sin* 25: 737-746

Chapter 4: Mucus rheology, response to salt addition, and resultant droplet formation

Introduction:

In chapter 3, bench-top systems for droplet generation were created and compared to existing literature for validation. As the overall focus remains on bioaerosols and methods to prevent their formation, the next step involves investigating the second hypothesis of this thesis, which states:

> Mucus viscoelasticity will influence droplet formation by shear forces, with increased stiffness yielding fewer droplets in total.

This hypothesis will be explored by examining the physical properties of the airway lining fluid (ALF), the role those properties play in droplet formation, and the means of altering those properties to reduce or prevent droplet generation. The properties of interest are the surface tension at the air-ALF interface and the viscoelasticity of mucus. However, based on the theoretical work performed by Moriarty and Grotberg[16] as well as the experimental results published by Edwards et al.[17] and Watanabe et al.[18] changes in surface tension, which tends to act as a stabilizing force, do not significantly influence droplet formation (for the range of physiologically relevant surface tension values, as found in the upper airways). Furthermore, as Edwards et al. reported, changes in viscoelasticity appeared to reduce expelled droplet numbers. Mucus viscoelasticity is therefore of primary interest.

Background:

Mucus is the primary component of ALF, and provides a protective coating which maintains hydration and serves as a physical barrier to foreign material. It can be found in the pulmonary system, eyes, gastrointestinal tract and other moist, sensitive areas of the body[1]. It is composed primarily of water and mucin macromolecules and is characterized by its viscoelastic

response to shear forces, demonstrating thixotropic behavior. This response is a function of its composition, and is specifically tuned to optimize the protective properties of mucus. Collection of adequate quantities of healthy pulmonary mucus has generally proven a major challenge, as it is produced in low volume, and covers the surface area of the pulmonary system. Typically, it has been obtained through sputum induction, which involves inhalation of salt-containing aerosols which alter its physical properties. Therefore substitutes for healthy pulmonary mucus have been investigated, including animal-derived sources and human cell culture models.[3] Comparisons have also been made to disease-state pulmonary mucus (e.g. chronic obstructive pulmonary disorder (COPD), cystic fibrosis (CF), etc.).[4,5]

Numerous studies have been performed on the viscoelasticity of mucus (healthy when possible, as well as diseased state) and mucus substitutes. In particular, Lutz et al. (1973)[19], King et al. (1977)[20], Crowther et al. (1984)[2]and Lethem et al. (1990)[21] contributed to the development of methods for measuring mucus viscoelasticity as well as characterizing its properties. Their work formed the foundation for investigating the changes in disease-state mucus and mucus functionality. For example, Lethem examined the properties of CF mucus and determined how the observed changes in viscoelasticity were the result of variations in the glycoprotein network. Crowther and Marriott demonstrated the viscoelastic sensitivity to ion concentration of pig gastric mucus, in particular cations such as calcium (although they only looked at very small ion concentrations).They saw an increase in viscoelasticity in response to calcium exposure[2], and posited a charge-shielding mechanism to explain it[13]. This is of particular relevance to the current work, as ions present a means of altering mucus viscoelasticity. However, the concentration range will be expanded and applied to whichever mucus source is found to be most

suitable. Once that is accomplished, bioaerosol formation as a function of mucus viscoelasticity can then be measured using the simulated cough machine developed in chapter 3.

Mucus and viscoelasticity:

As discussed in chapter 2, mucus is comprised of chain-like glycoproteins (specifically MUC5b and MUC5ac in pulmonary mucus). The fluid properties of mucus arises from the interaction of these molecules: non-covalent bonds, disulfide bridges and simple entanglement produce a macroscopic network in constant flux which can also elastically deform under stress, storing potential energy in a mechanical "spring-like" fashion (Figure 4.1). Each mucin chain can act as a pseudo-spring, so that energy is stored across the entire network; however the mucin chains are also in motion relative to each other and this motion gives rise to viscous flow. Hence, mucus exhibits behaviors similar to both viscous fluids and elastic solids.

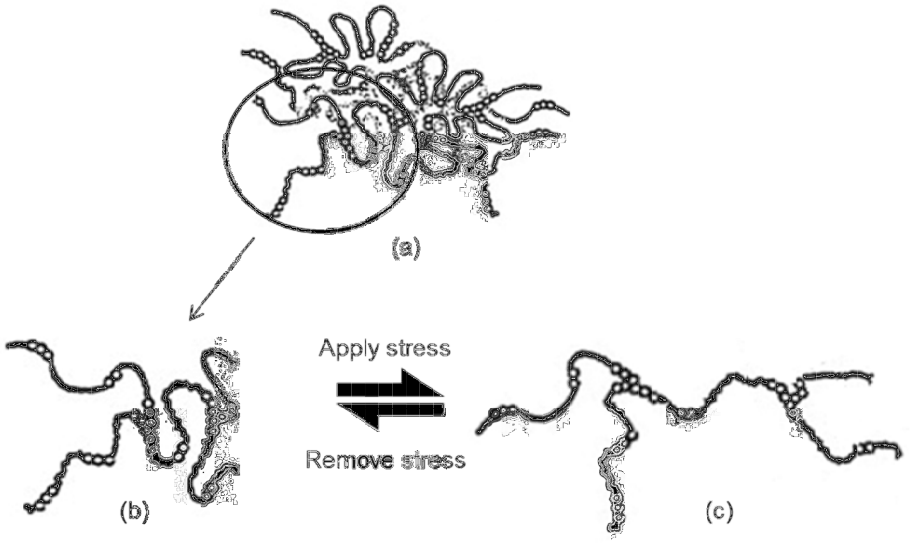

Figure 4.1: (a) Overall mucin network (b) "Relaxed" mucin chains (c) Stretched mucin chains (storing energy elastically)

When a shear stress is applied to the mucin network, the mucin chains are stretched, creating strain. The mucins may also slide along each other, dis-entangling and flowing in the direction of the stress, reducing tension in the system. Over a longer period of time, the inter-mucin bonds may break (and reform), which further reduces overall strain. If the applied stress is removed, the system can relax; however the final state will differ from the pre-stress state depending on the relative amounts of elastic deformation and flow, as well as the overall time-scale. In other words, the applied stress will be correlated with both the strain (as in an elastic solid) and the rate of strain (as in a viscous, or Newtonian, fluid). The study of such complex fluid flow is called rheology. Rheometers are used to measure the viscoelastic properties of materials. Samples are loaded into a particular geometry which is attached to the rheometer: there are many types of geometries, including plate/plate, cone and plate, and couette, each of which consists of at least two components and which is designed to apply shear force to the sample. An example of a cone and plate geometry is shown in Figure 4.2.

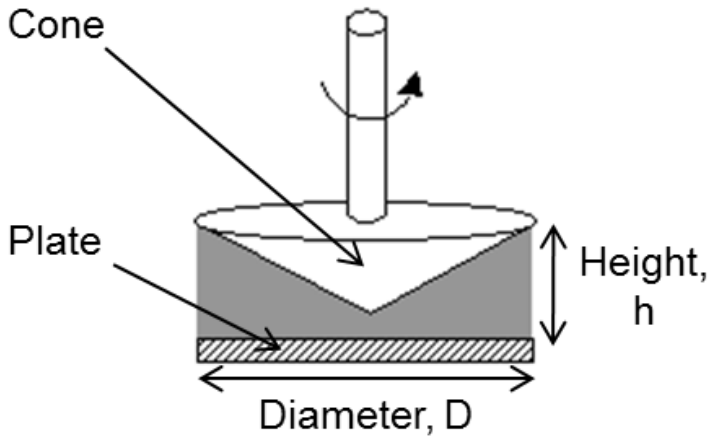

Figure 4.2: Cone and plate geometry

As in Figure 4.2, sample is loaded between the cone and plate, and care is taken to insure that no air bubbles or gaps are present, nor that any excess material is outside the diameter of the cone. The cone is rotated with respect to the plate and the applied stress (the torque on the spindle attached to the cone over the interfacial area) is measured along with the rotational displacement. Strain is calculated as the displacement distance divided by the sample height: one advantage of the cone and plate geometry is that the sample is subjected to uniform strain (for a fixed displacement angle, the displacement length is a function of radius, and the sample height is designed to be a function of radius as well, resulting in uniform strain).

The rheometer can be operated in two basic modes: a rotational or direct shear mode in which the cone is rotated at a set speed or to a set displacement; and an oscillatory mode, in which the cone oscillates back and forth with a particular frequency. The former is used to generate information about how the sample responds to fixed stress, strain, or shear rate – for example, the shear-thinning behavior of mucus is observed with this method – but it may be destructive to the sample's networked structure. The latter is used to ascertain the importance of time-scales and measure viscoelastic properties without permanently altering the network structure. During an oscillatory experiment, a sinusoidal stress or strain is applied to the sample and the resulting strain/stress is measured (an example is shown in Figure 4.3). The phase lag between the stress and strain curves is dependent on the sample type: a Newtonian fluid would be 90 degrees out of phase, whereas an ideal, elastic solid would be perfectly in-phase. The phase lag for complex (non-Newtonian) fluids will fall somewhere between 0 and 90 degrees. The viscoelasticity of the sample can then be quantified as a complex number, defined as the complex (dynamic) modulus, G^* (equation III), with phase angle δ.

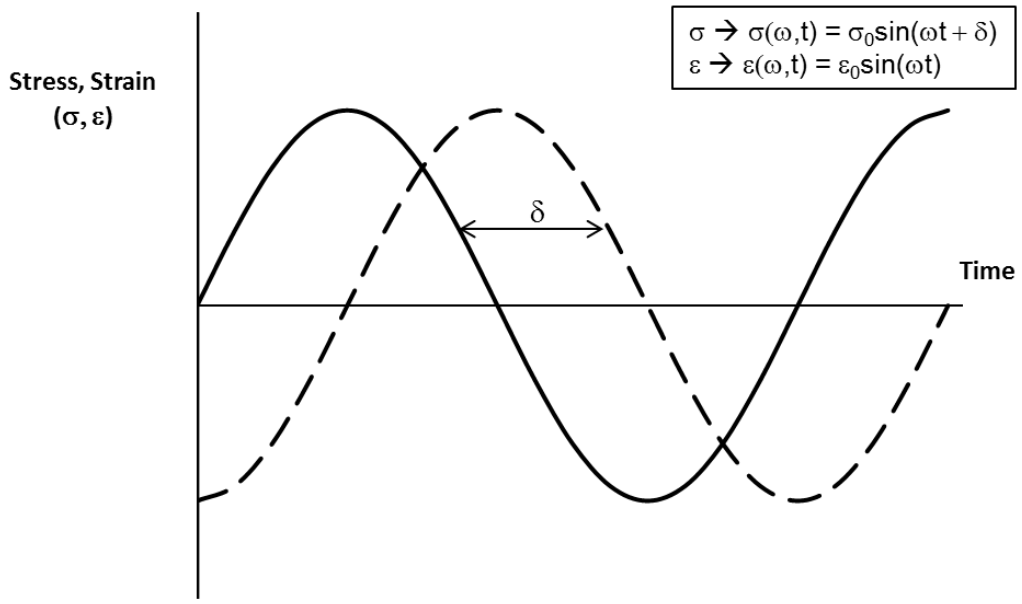

Figure 4.3: Example of sinusoidal applied stress and strain (at frequency ω) with phase lag

$$\sigma = \mathrm{Im}(\sigma_0 e^{i(\omega t-\delta)}) = \mathrm{Im}(\sigma_0 e^{i\omega t} e^{i\delta}) \qquad \text{(I)}$$

$$\varepsilon = \mathrm{Im}(\varepsilon_0 e^{i\omega t}) \qquad \text{(II)}$$

$$G^* \equiv \frac{\sigma}{\varepsilon} = \frac{\sigma_0}{\varepsilon_0} e^{i\delta} = \frac{\sigma_0}{\varepsilon_0}\cos(\delta) + i\frac{\sigma_0}{\varepsilon_0}\sin(\delta) \qquad \text{(III)}$$

$$G' \equiv \frac{\sigma_0}{\varepsilon_0}\cos(\delta) \qquad \text{(IV)}$$

$$G'' \equiv \frac{\sigma_0}{\varepsilon_0}\sin(\delta) \qquad \text{(V)}$$

$$G^* = G' + iG'' \qquad \text{(VI)}$$

$$\frac{G''}{G'} = \tan(\delta) \qquad \text{(VII)}$$

Where: σ = Stress

ε = Strain

δ = Phase Lag

ω = Frequency

t = Time

G* = Complex Modulus

G' = Storage Modulus

G" = Loss Modulus

The components of equation (III) can be further defined as the storage modulus, G' (equation IV) which is a measure of the elastic response of the sample; and the loss modulus, G" (equation V) which is a measure of its viscous response. Rewriting equation (III) with these terms results in equation (VI). The magnitude of G^* is a measure of the overall "stiffness" of the system (i.e. its resistance to deformation), and the ratio of G" to G' (equation VII) quantifies the amount of energy dissipated by the material to that stored when deformed.

Mucus sources:

Due to the difficulty in acquiring healthy pulmonary mucus, which is typically obtained through sputum induction via hypertonic salts[6] – a process which would invalidate further testing on mucus exposure to cations – alternative mucus sources were investigated. Alternative sources were selected from the following categories: mimetic gels (designed to mimic mucus); animal-derived mucins; and human sources. Table 4.1 lists the viscoelastic properties of healthy human

pulmonary mucus reported in the literature. For all samples, viscoelasticity was measured with an AR-G2 rheometer with cone and plate geometry (TA Instruments, New Castle, DE) and results were compared to healthy mucus. Results for all samples are shown in Figures 4.4 (complex modulus) and 4.5 (loss tangent).

Table 4.1: Reported values for viscoelasticity of healthy pulmonary mucus[13]

Property	Value
Viscoelasticity	
- Complex Modulus	2-10 Pa
- Loss Tangent	0.2-0.4

Mimetics:

Various natural and synthetic gums and gels have been explored in the literature, such as guar gum, locust bean gum and sodium alginate[7]. Sodium alginate is a long-chain molecule which is cross-linked by calcium to form a gel. The gel properties are dependent on the alginate concentration as well as the calcium concentration used to crosslink the sample, although these parameters are limited by solubility and the number of available cross-linking sites. The closest match to healthy mucus was obtained from a 2% w/w alginate solution cross-linked by 1 mM calcium chloride – viscoelastic results are presented in Figures 4.4 and 4.5.

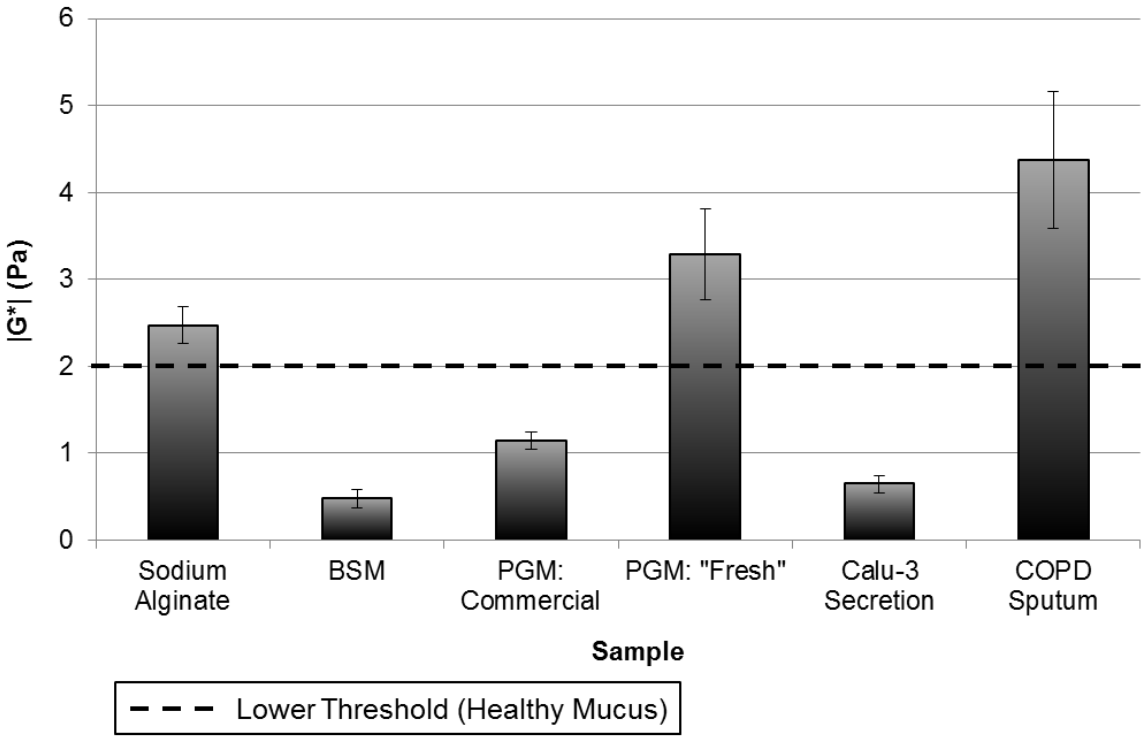

Figure 4.4: Complex modulus (magnitude) for alternative mucus sources

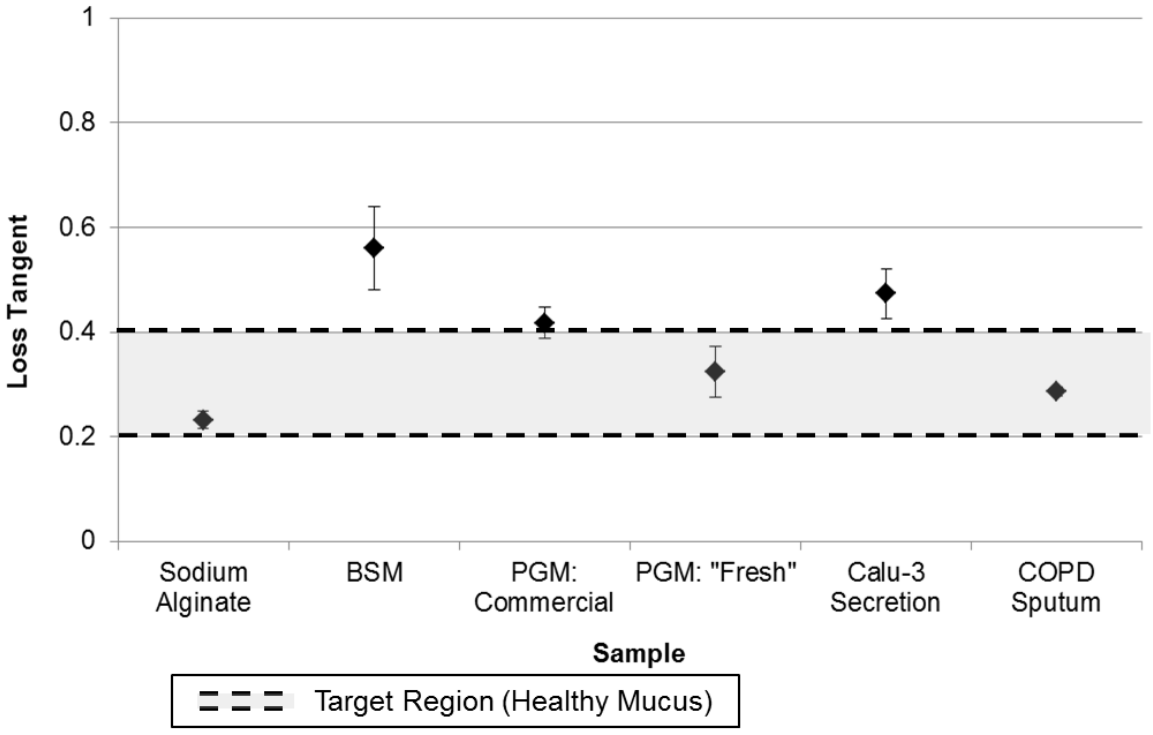

Figure 4.5: Loss tangent values for alternative mucus samples

Ultimately, due to different chemical structures (alginate's chemical structure is shown in Figure 4.6) and interaction dynamics, mimetics are only a useful comparison for particular viscoelastic "states" (i.e. matching viscoelastic properties under specific conditions). Their response to changes in the conditions (varying frequency, for example) or to the addition of ionic agents and other compounds will not match the response of mucus to those same changes.

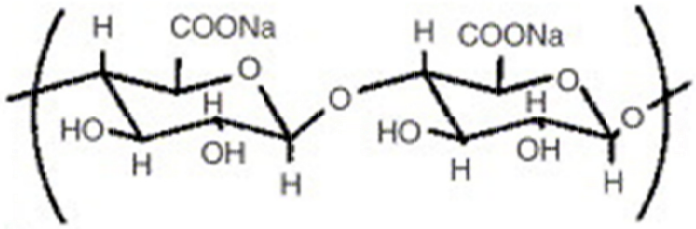

Figure 4.6: Chemical structure of sodium alginate[16]

Animal-derived sources:

Many different animal sources of mucus have been explored, including submaxillary, gastric and cervical mucins extracted from pigs or cows. Similar for humans, pulmonary sources are low volume, and therefore rarely considered. Purified bovine submaxillary mucins (BSM) (MP Bio, Solon, OH) are commercially available as lyophilized powders, as are porcine gastric mucins (PGM) (Sigma Aldrich, St. Lois, MO), although the specific procedures used for processing the samples were not released by the manufacturers. Additionally, porcine gastric mucus was collected from freshly harvested pig stomachs and purified following procedures outlined in reference 8. Results are shown in Figures 4.4 and 4.5. BSM was the poorest match to healthy human mucus, and the commercially available PGM was only moderately better. The

freshly purified PGM was a strong match, but unfortunately the collection process was prohibitively time-intensive for the amount of material produced (3-4 weeks were required to produce a few hundred milligrams of final product).

Human sources:

Two human-based sources of pulmonary mucus were examined: mucus secreted from Calu-3 cells (which are cultured from human airway epithelial cells)[9]; and sputum obtained from patients suffering from chronic obstructive pulmonary disorder (COPD). Calu-3 cell cultures produced a few hundred microliters of mucus on a weekly basis, so several cultures were harvested concurrently and the secretions pooled over time to produce useable quantities. COPD is characterized by excessive production of pulmonary mucus (with volumes exceeding tens of milliliters per day from a single individual). Unlike in cystic fibrosis (CF), in which much thicker, stiffer mucus is produced, COPD mucus has been found to more closely match healthy mucus[10]. Sputum samples were collected by a third party and provided for research purposes: 10 patients provided a sputum sample daily for five days. All samples were kept frozen at -80^{o}C until needed, at which point individual samples were thawed for testing as needed. Results are included in Figures 4.4 and 4.5: Calu-3 secretions were a poor match for healthy mucus; however, as expected, COPD sputum was a very strong match. COPD was selected for further characterization and experimentation.

Large variations in viscoelasticity were observed between COPD sputum samples provided by different individuals, specifically in the complex modulus (inter-patient sample data is shown in Figure 4.7). The mean value for complex modulus across all samples was 5.3 Pa. The relative standard deviation (RSD) was 58.6%. Much less variation was observed in the loss

tangent (mean: 0.253; RSD: 17.98%). Variations between samples provided by the same individual on different days were observed as well, however they tended to be smaller than the range observed across different individuals. Figure 4.8 shows the RSD in the complex modulus across samples collected over multiple days for each individual.

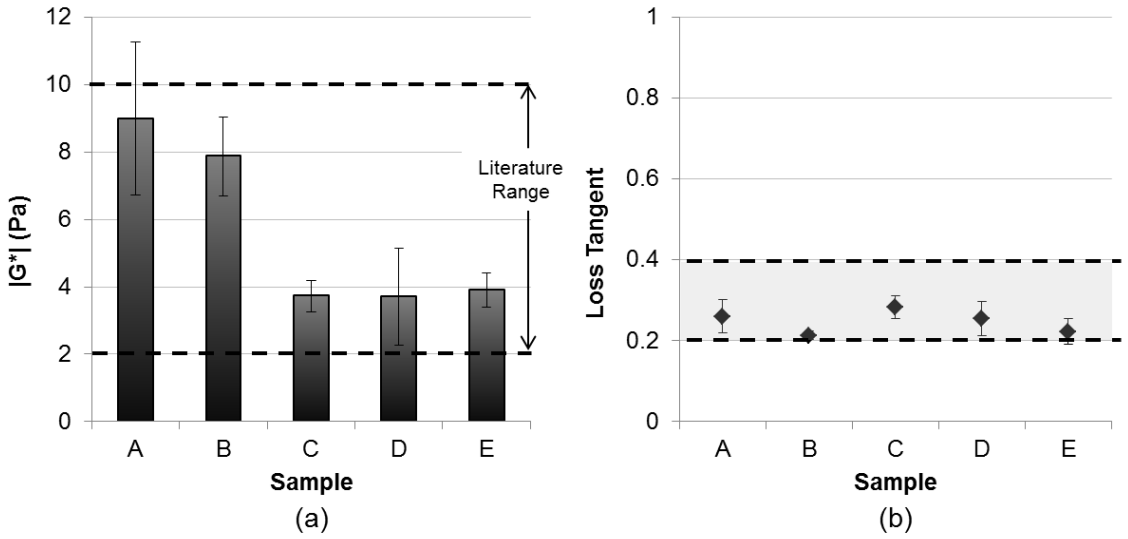

Figure 4.7: Inter-patient viscoelasticity in COPD sputum – (a) Magnitude of complex modulus; (b) Loss tangent

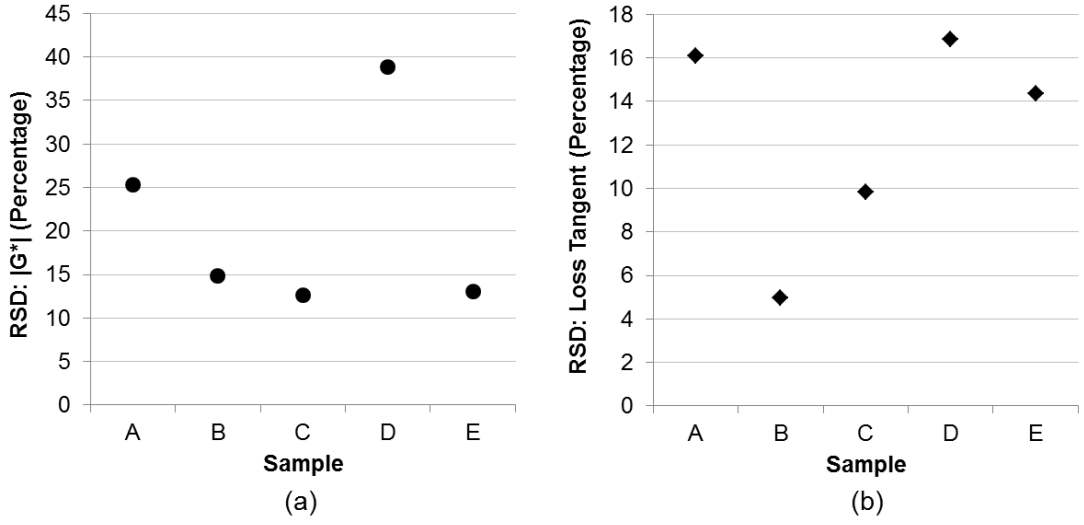

Figure 4.8: Intra-patient variation in COPD sputum – (a) RSD of complex modulus; (b) RSD of Loss tangent

As a result of the observed variation, samples were pre-screened and selected for viscoelastic parameters: samples were accepted for further testing provided the mean complex modulus was within one standard deviation of the overall sample mean (between 3 and 6 Pa). Samples outside this range were considered outliers for the purposes of further experimentation. Furthermore, for studies involving the effect of salt exposure, viscoelastic parameters were normalized against their baseline (untreated) values to aid in comparing results.

Bulk additives:

In order to explore the effect of cations on mucus viscoelasticity, different salts were added in bulk to COPD sputum samples at varying concentrations and the resulting viscoelasticity was measured. Four salts were investigated: calcium chloride, magnesium chloride, sodium chloride and potassium chloride (all obtained from Sigma Aldrich). Calcium and magnesium are divalent cations; sodium and potassium are monovalent cations. Results are shown in Figures 4.9 and 4.10: at low cation concentrations, decreases in the loss tangent and increases in the complex modulus (compared to baseline values) were observed. The effect was greater for the divalent cations compared to the monovalent cations. These changes indicate increased gel stiffness arising from increasing elasticity (larger complex modulus, smaller loss tangent). However, as the concentration was increased the response was reversed and ultimately the overall stiffness decreased, with greater losses in the storage moduli than loss moduli (smaller complex modulus, larger loss tangent). Variation in the results was reasonably large, typically between 10 and 20% RSD, with a few outliers, but this reflects the baseline variation in the sputum samples themselves in addition to any experimental error.

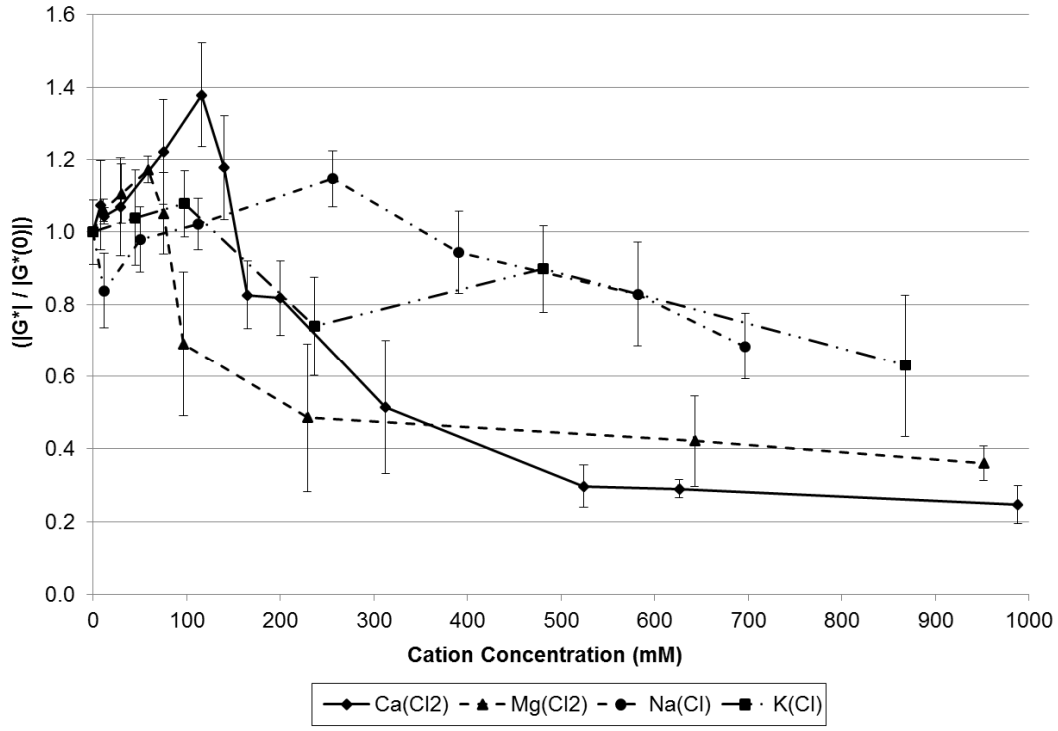

Figure 4.9: Normalized complex modulus versus cation concentration

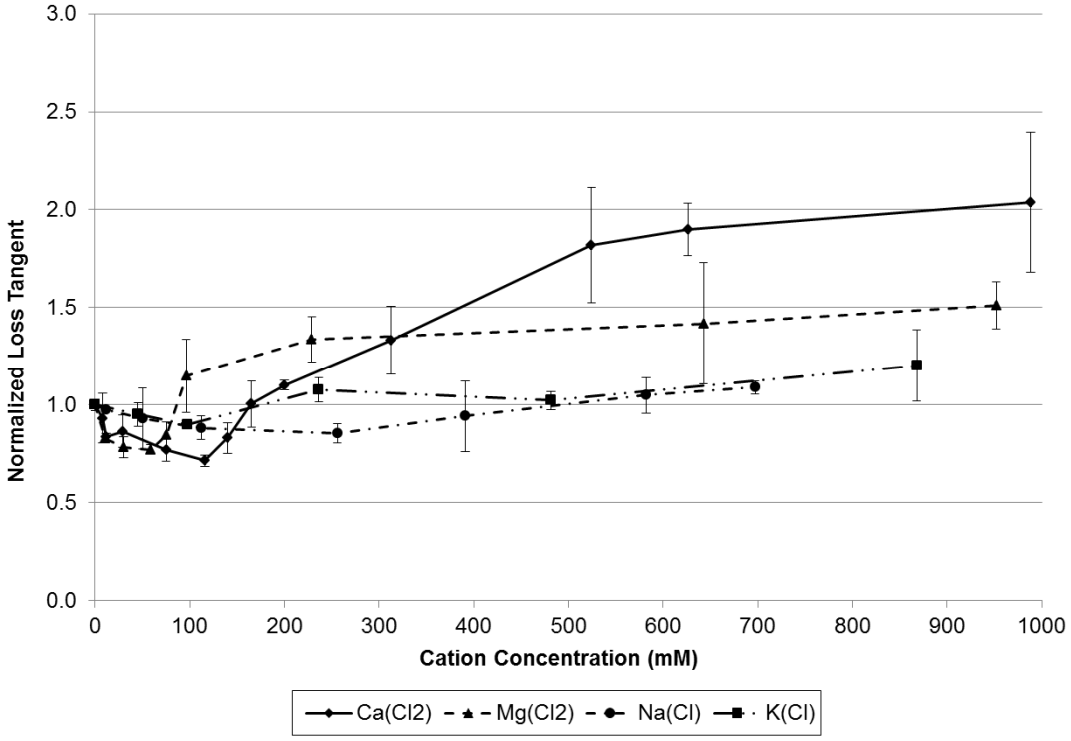

Figure 4.10: Normalized loss tangent versus cation concentration

The observed increases in stiffness at low cationic concentrations are the result of charge-shielding (Figure 4.11)[13]. Sialic acids attached to the mucin backbones are negatively charged and cause repulsion between mucins, but the presence of positively charged cations shields the negative charge between the mucin arms, reducing repulsion and allowing the mucins to associate more closely. This, in turn, allows for a higher entanglement density in the mucin network, which results in increased stiffness. However, as the cation concentration increases, the mucins continue to contract and ultimately condense into their pre-release state, disintegrating the network.[11-14]

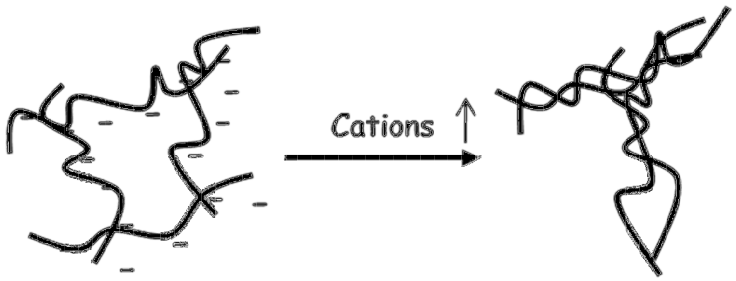

Figure 4.11: Example of increased mucin interaction as a result of cation-induced charge-shielding

Results:

In order to investigate the role of mucus viscoelasticity in bioaerosol formation, the salt-treated COPD sputum samples were also used in the simulated cough system developed in chapter 3. The samples were loaded by syringe in a particle free bio-hood and then spread over a fixed area. Cough-equivalent air flow was generated by a breathing simulator, and the resulting air stream was sampled at 28.3 sLMP by an exhalair system for particle measurement. Any droplets produced were assumed to be well-mixed with the air stream. Results are shown in Figure 4.12, however large variability was observed for virtually all samples. In general, the

droplet concentration tended to decrease at low cation concentration and then rise significantly as cation concentrations were increased. The largest decreases were observed for the divalent cations (calcium and magnesium). This appears to match the viscoelastic response to cation concentration previously observed.

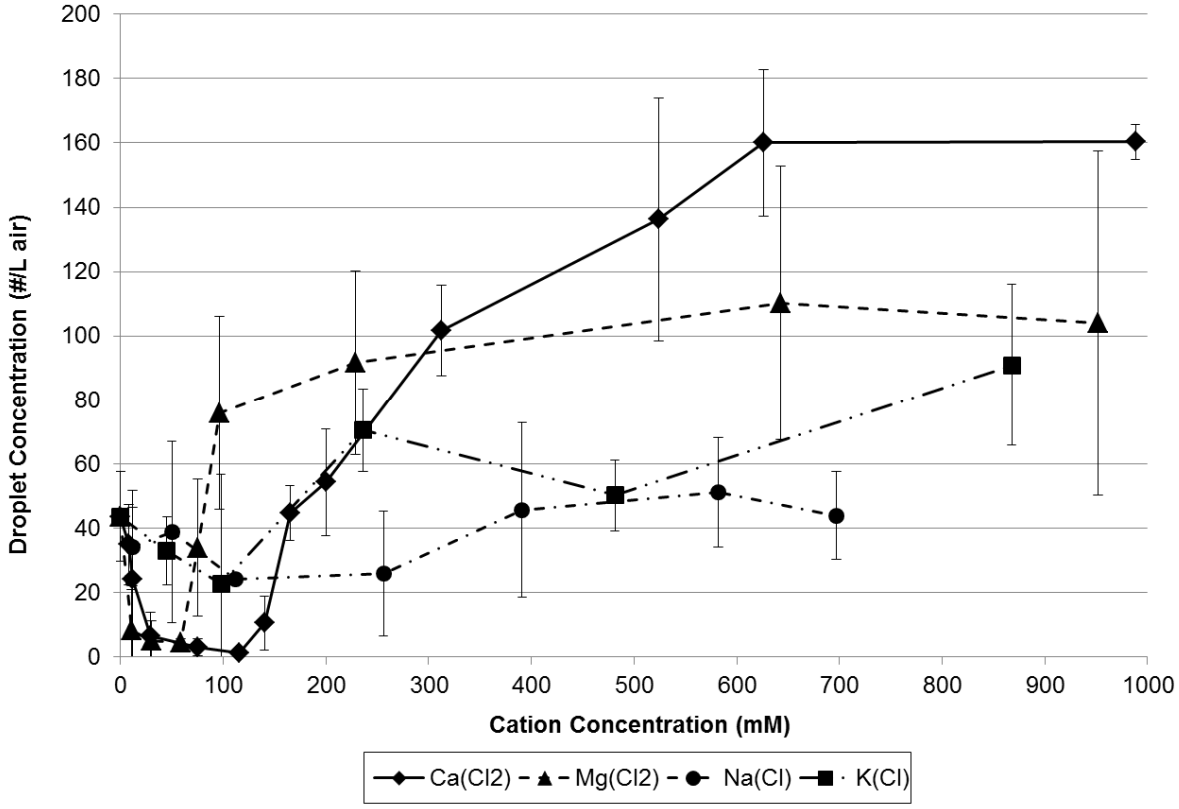

Figure 4.12: Droplet concentration versus bulk sample cation concentration

Comparing droplet concentration to the normalized complex modulus for each sample indicates a strong inverse correlation (correlation coefficient of -0.96) between particle generation and viscoelasticity (Figure 4.13), with over 90% (R^2 greater than 0.9) of the variance in droplet concentration accounted for by the normalized complex modulus. However, as previously discussed, the intra-sample variability in both parameters is still quite large.

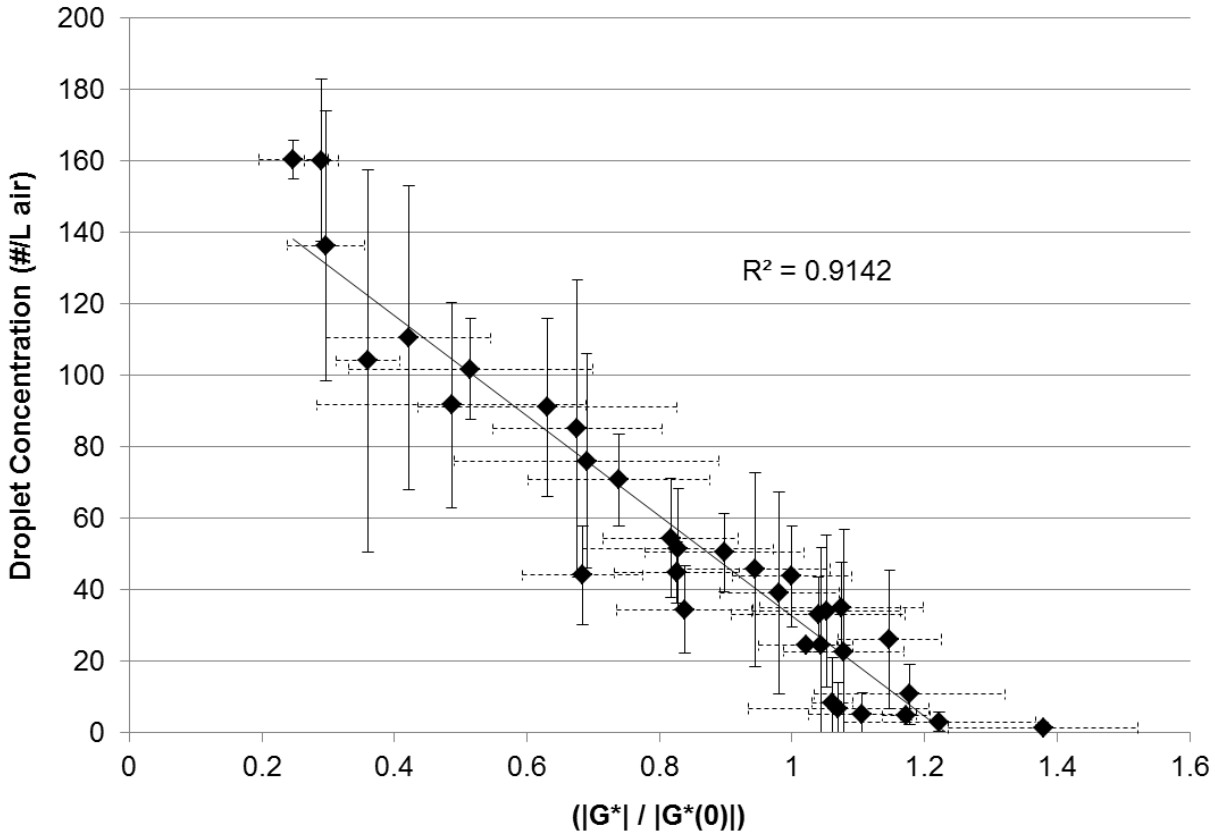

Figure 4.13: Scatterplot of droplet concentration versus normalized complex modulus ($n \geq 3$ for all samples)

To determine whether the intra-sample variability would significantly alter the results, the data from every individual experiment (rather than the average over multiple replicates) was pooled and the droplet concentration versus complex modulus was plotted (Figure 4.14). Unsurprisingly, the sample noise can be seen as a direct influence on the variance (R^2 of 0.79) as well as the overall correlation strength (correlation coefficient of -0.89), which is still strong. The same overall trend is still apparent.

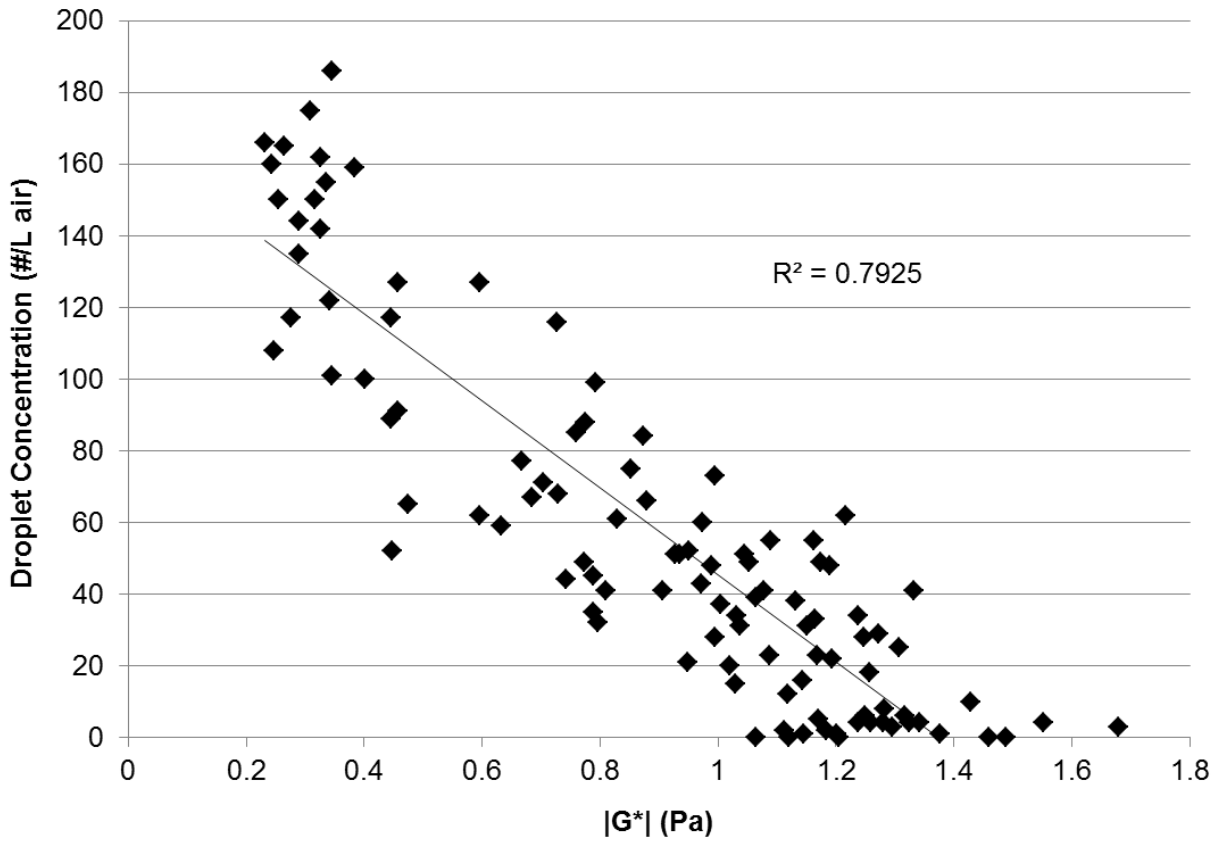

Figure 4.14: Scatterplot of droplet concentration versus complex modulus for individual experiments

Conclusion:

After extensive exploration of available alternatives to healthy human pulmonary mucus, COPD sputum was selected as the best viscoelastic substitute. Freshly purified and reconstituted PGM was also a reasonable fit; however time and manufacturing constraints limited its availability. Inter- and intra-patient variability in the viscoelasticity of the COPD sputum samples were examined, along with the bulk addition of various salts: normalization was used to determine and compare changes in viscoelasticity.

Changes in viscoelasticity were observed as a result of salt exposure: the magnitude and direction of such changes were dependent on cation concentration as well as cation valency. This

response was consistent (at low cation concentration) with the work performed by Crowther and Marriott, and is attributed to the same charge-shielding mechanism they proposed. The treated and untreated samples were also used in a simulated cough system to measure droplet production. Droplet concentration was found to be inversely correlated with the complex modulus of the sample. These results confirm the second hypothesis: that altering the viscoelasticity of mucus (in this case through addition of cationic agents) would influence shear-induced bioaerosol generation.

References:

1. Lai, S.; Wang, Y.; Wirtz, D.; Hanes, J (2008) *Adv. Drug Deliv. Rev*. 61(2): 86-100
2. Crowther, S.; Marriott, C. (1984) *J. Pharm. Pharmacol*. 36(1): 21-26
3. Tippe, A.; Korbel, R.; Ziesenis, A.; Heyder, J. (1998) *Scand. J. Clin. Lab. Invest.* 58(3): 259-264
4. Galabert, C.; Jacquot, J.;Zahm, J.; Puchelle, E. (1987) *Int. J. Clin. Chem*. 164: 139-149
5. Lopez-Vidriero, M.; Reid, L. (1978) *Br. Med. Bull*. 34: 63-74
6. Sims, D.; Westfall, J.; Kiorpes, A.; Horne, M. (1991) *Biotech. Histochem*. 66: 173-180
7. Zayas, G.; Dimitry, J.; Zayas, A.; O'Brien, D.; King, M. (2005) *BMC Pulm. Med.* 5: 11
8. Gong, D.; Turner, B.; Bhaskar, K.; LaMont, J. (1990) *Am. J. Physiol*. 259: 681-686
9. Lehr, C. (2002) *Cell Culture Models of Biological Barriers: In vitro Test Systems for Drug absorption and Delivery* Ch. 13: 211-227
10. Rogers, D.; Lethem, M. (1997) *Airway Mucus: Basic Mechanisms and Clinical Perspectives*, Ch.11-12: 275-326
11. Verdugo, P.; Deyrup-Olsen, I.; Aitken, M.; Villalon, M.; Johnson, D. (1987) *J. Dent. Res*. 66(2): 506-508
12. Marriott, C.; Litt, M. (1978) *J. Pharm. Pharmacol.* 30: 9p
13. Marriott, C.; Shih, C.; Litt, M. (1979) *Biorheology* 16(4-5): 331-337
14. Lai, S.; Wang, Y.;Cone, R.;Wirtz, D.; Hanes, J. (2009) *PLoS One* 4(1): 4294
15. Macklem, P. T.; Proctor, D. F.; Hogg, J. C. (1970) *Respir Phsysiol*.8:191–203
16. Moriarty, J.; Grotberg, J. (1999) *J. Fluid Mech*. 397: 1–22
17. Edwards, D.; Man, J.; Brand, P.; Katstra, J.; Sommerer, K.; Stone, H.; Nardell, E.; Scheuch, G. (2004)*PNAS* 101(50): 17383-17388
18. Watanabe, W.; Thomas, M.; Clarke, R.; Klibanov, A.; Langer, R.; Katstra, K.;Fuller, G.; Griele, L.; Fiegel, J.; Edwards, D. (2007)*J Colloid Interface Sci.* 307(1): 71–78
19. Lutz, R.; Litt, M.; Chakrin, L. (1973) *Rheology of biological systems* 119
20. King, M.; Macklem, P. (1977) *J. Appl. Physiol*. 42: 797-802
21. Lethem, M.; James, S.; Marriott, C. (1990) *Am. Rev. Respir. Dis.* 142: 1053-1058

Chapter 5: Preventing bioaerosol transport by modifying mucus viscoelasticity

Introduction:

In Chapter 4, a correlation between mucus viscoelasticity and droplets generated by cough-induced surface-shearing was established and confirmed the second hypothesis. Mucus viscoelasticity was modified through cationic exposure. These results were in agreement with published work performed by Edwards et al.[9], Watanabe et al.[10] and Clarke et al.[11] and can be applied *in vitro* to determine how modifying mucus viscoelasticity influences the transport of pathogens via bioaerosols. Pathogen transport will be established for both bacteria and viruses, after which the effect of cationic treatment of infected mucus will be explored in order to test the third hypothesis, which states:

> Reducing the number of bioaerosols generated decreases the probability of pathogen transport, and therefore the transmission of infection.

Calcium was selected as the appropriate cation to modify the viscoelasticity of COPD sputum based upon the increased sensitivity observed in the previous chapter. This will be investigated using a modified version of the simulated cough system previously developed.

Background:

Attempts to collect pathogen from expelled droplets have advanced significantly from the large-droplet impaction studies of Duguid[12] in the 1940s. Modern methods include impactors, which are designed such that the air flow path enters through one end of the device and must curve sharply to pass around a large dish or plate (or a series of plates), before exiting out the other end. This creates the potential for inertial impaction (onto the plate) of particles within the air stream that are too aerodynamically large to follow the air flow path around the dish. Multiple

stages with varying size cut-offs can be used to determine the size distribution. Liquid impingers operate in a similar fashion, but particles are collected in liquid, rather than deposited directly onto plates.

Airborne transmission has been successfully demonstrated between animals: in 1962 Riley et al.[13] published a study in which guinea pigs that were exposed to air from a tuberculosis ward became infected. Autopsies of the infected guinea pigs revealed that only a single infectious droplet was necessary to initiate infection. In 2011, A. Nalca and D. Nichols[14] published results demonstrating bioaerosol transmission of rabbit pox between healthy and infected rabbits. Unpublished work by members of Pulmatrix[15], Inc. has also shown disease transmission by aerosol in cattle and pigs, as well as a reduction in transmission via cationic treatment, however no direct measurements of the properties of the animals' airway mucus was possible. Hence the need for an *in vitro* system to monitor pathogen transmission under controlled settings in which the mucus properties can be measured and treatment effects analyzed.

Test system development:

The simulated cough system presented in chapters 3 and 4 was modified as follows: the Exhalair system (for measuring droplet number and size) was replaced by a single-stage viable Anderson Cascade Impactor (viable-ACI, Thermo Scientific, Waltham, MA). Viable-ACIs can be single- or multi-stage, and are used to characterize the number, aerodynamic size and size distribution of airborne, biologically-active particles. The impactor was placed approximately 15 centimeters downstream from the pseudo-trachea with a trap between them to prevent sample material from being pushed into the impactor. A schematic of the complete system is shown in

Figure 5.1. An ULPA filter was placed after the impactor to collect any droplets which did not deposit and remained airborne.

The mucus sample was loaded into the pseudo-trachea within a particle free biohood, and a petri dish, containing appropriate receptor material, such as agar gel or cell media, was placed in the impactor. The cough maneuver was then initiated: any droplets formed travel to the impactor, where they may contaminate the receptor material within the petri dish. Afterwards, the petri dish was removed and the receptor material was either placed directly into an incubator (agar plates) or removed and placed over cell cultures (cell media). These were subsequently observed for the presence of pathogens.

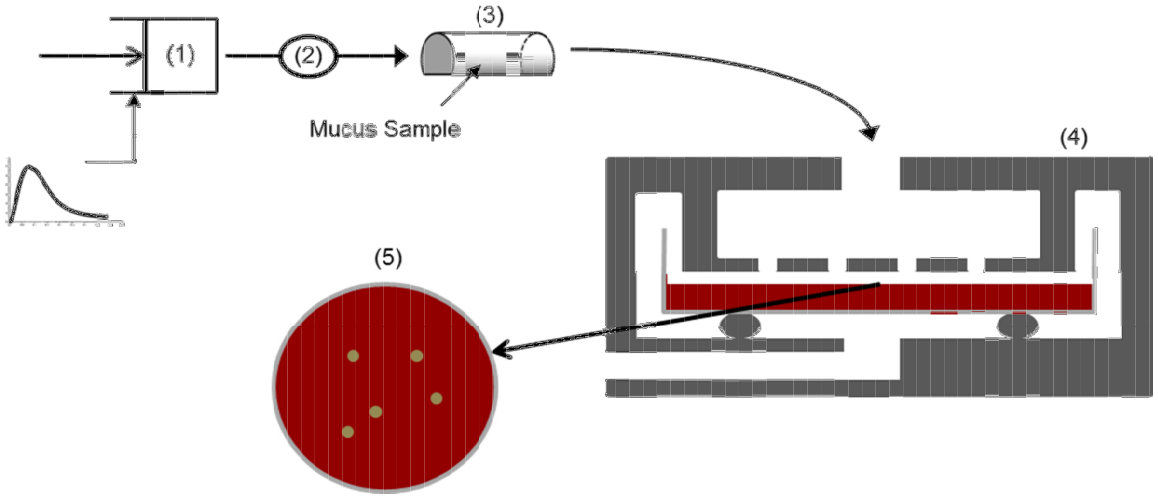

Figure 5.1: Schematic of experimental transmission system: (1) Breathing Simulator;(2) ULPA Filter; (3) Pseudo-trachea; (4) Impactor; (5) Contaminated petri dish with agar/media

Method development:

COPD sputum was used for all mucus samples. All calcium-treated mucus samples were exposed to a final concentration of 116 mM calcium, which corresponded to the largest increase in complex modulus and largest decrease in loss tangent (Figure 5.2). The viscoelasticity of all samples (calcium-treated and untreated) was measured prior to each experiment to confirm agreement with previous results.

An unknown bacterium was present in the raw mucus samples. Plating "neat" sputum on chocolate agar and incubating at 32^{o}C for 24 hours resulted in the observation of hundreds of CFU. Sputum was serially diluted with phosphate buffered saline and plated. CFUs of the unknown bacteria were observed down to a dilution of 1:1000. Calcium-treated sputum yielded similar results, indicating that there was no direct effect of calcium-treatment (at the selected concentration) on bacteria quantity; however treatment with an anti-bacterial Penicillin-Streptomycin ("pen-strep") solution was able to eliminate the observed bacteria.

The presence of native bacteria in the sputum samples prevented direct addition of known bacteria for experimental purposes, as all results would be contaminated by the native bacteria. However, treatment of the mucus with pen-strep was not a functional solution. An effective dose required too large a volume and produced a diluting effect on the mucus samples. It would also have required that any subsequently added bacteria be resistant to both penicillin and streptomycin.

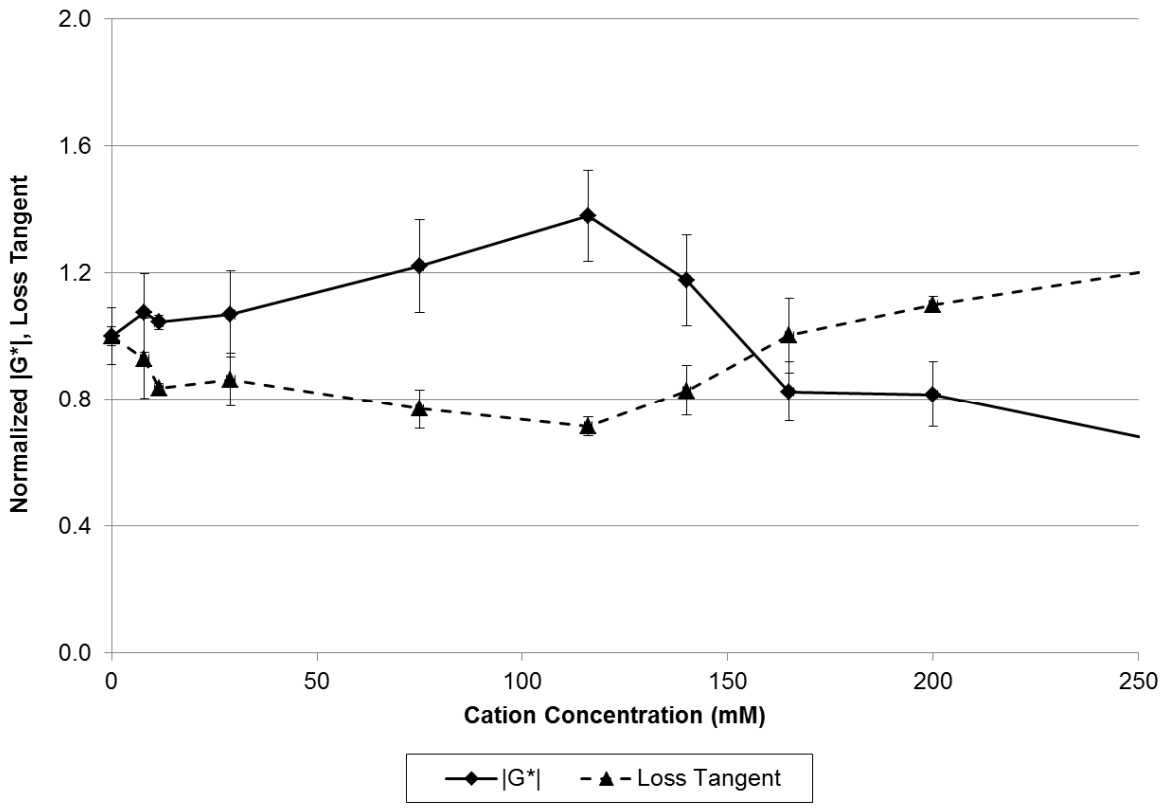

Figure 5.2: Changes in COPD sputum viscoelasticity resulting from calcium treatment

The native bacteria did present an opportunity to test the system for proof-of-concept with a simple positive/negative outcome (i.e. bacteria is either present or not present for a given mucus sample or condition). Three conditions were tested: no mucus (to check for background contamination), untreated mucus (to establish positive bacterial transport) and calcium-treated mucus (to determine effectiveness of cationic treatment). Each sample was loaded into the pseudo-trachea and spread over a fixed area before initiating the cough. Chocolate agar plates were used in the impactor to collect droplets (and enable the growth of any bacteria that reached them). The plates were incubated at 32^{o}C for up to 48 hours post-exposure. They were then observed for bacterial growth and CFUs were counted by hand. Results are shown in Figure 5.3.

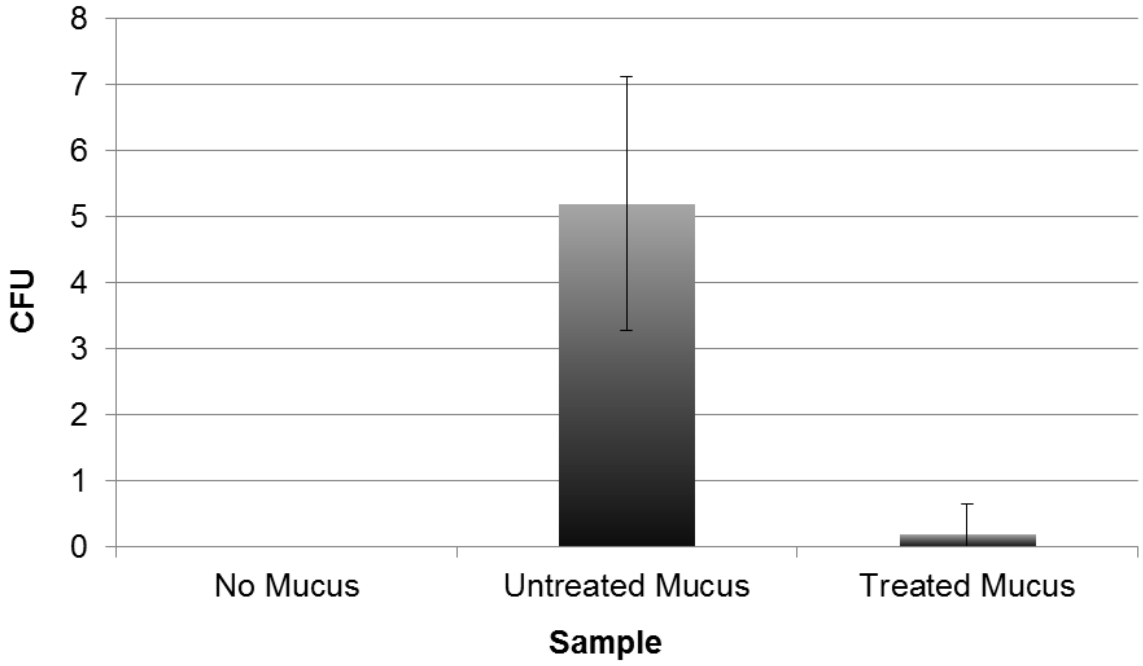

Figure 5.3: CFU of native bacteria observed 48 hours after cough exposure

As expected, when no mucus was used, no bacteria were observed on the agar plates, confirming a clean, uncontaminated background. When untreated mucus was tested, a small number of CFU were observed (5.2±1.9 CFU), indicating that at least a few bacteria were successfully transported via droplets and thereby providing a positive control for the system. When the mucus was treated with calcium, fewer CFU were observed (0.2±0.45 CFU) – four out of five replicates did not show any CFU at 48 hours. A t-test confirmed that the difference observed between the sample groups is statistically significant ($p < 0.0024$). Hence, the proof-of-concept for the simulated cough and impactor system was successful; furthermore, cationic treatment of mucus (to increase viscoelasticity) was demonstrated to reduce bacterial transport via airborne droplets.

Viral Transport:

Human rhinovirus (HRV) was used to examine viral transport: it was selected due to its prevalence as well its robustness. HRVs are considered the primary cause of the common cold, and are amongst the most common viral pathogens in humans. They can infect both the upper and lower respiratory tract, although they are primarily an upper respiratory tract disease. HRVs grow optimally at 31-33^{o}C (which is the typical temperature in the upper airways). They are extremely small, with a diameter of approximately 30 nanometers.[4]

The first step in an HRV infection begins when the virus attaches to Inter-Cellular Adhesion Molecule 1 (ICAM-1), a surface protein found on epithelial cells (Figure 5.4). This attachment occurs rapidly after exposure, typically occurring within 15 minutes, and causes a conformational change in the virus which triggers the release and transport of viral RNA into the cell,[5] however, symptoms do not typically appear for another 1 to 4 days after infection. HRV remains functionally intact in solution, at room temperature, for over an hour. This is significant, as it allows sufficient time for sample preparation and experimentation (as compared to influenza, which degrades much more rapidly and would require accelerated experimental protocols).

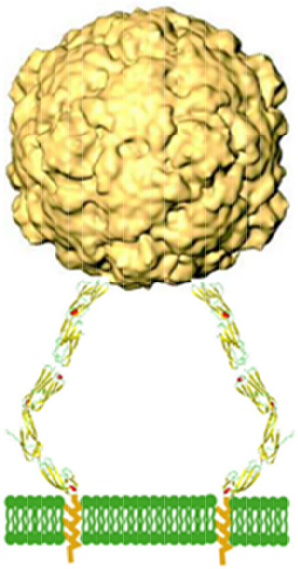

Figure 5.4: HRV attached to a cell via the surface protein ICAM-1.[6]

In order to create a reference standard for cell death following viral exposure, cell cultures of an HRV-sensitized HeLa phenotype (selected for increased expression of ICAM-1) were exposed to HRV at varying multiplicity of infection (MoI) – the ratio of virions to cells – and subsequently observed for cell death over 96 hours. This resulted in a set of data involving the time-to-death of cell cultures at known MoI which could be referenced against future experiments to approximate the amount of virus that cells had been exposed to (using only the time of death post-exposure). Results are included in Table 5.1. Additionally, to test whether calcium treatment would directly influence HRV activity, HRV was added to 116 mM solutions of $CaCl_2$ in cell culture media and incubated at room temperature for 15 minutes. The solution was then directly added to HRV-sensitized HeLa cell cultures. Cell death followed in accordance with the equivalent reference standard, indicating that the HRV remained active in the presence of $CaCl_2$.

Results:

Calcium-treated and untreated sputum samples were spiked with approximately 10^7 HRV (Rhinovirus 16, ATCC, Manassas, VA) virions and gently agitated for 10 minutes to allow for complete mixing. No changes were observed in mucus viscoelasticity within 30 minutes of virus exposure (which was the length of time needed to prepare the samples, then load and run the simulated cough system). Magnesium fortified cell-culture media was placed in petri dishes and loaded into the impactor. After cough exposure, the contaminated media was placed on HRV-sensitized HeLa cell-cultures. The following conditions were tested: untreated sputum without virus ("neat"); untreated sputum with virus; and calcium-treated sputum with virus. Exposed cells were incubated at 32°C for 96 hours post-exposure, and assessed visually (via microscopy) every 24 hours for cell death; results are shown in Table 5.1.

Table 5.1: HeLa cell culture response to cough-contaminated media over 96 hours

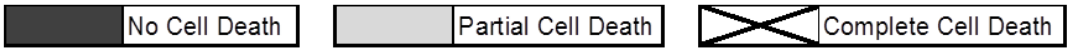

Sample	0 hr	24 hr	48 hr	72 hr	96 hr
Reference (MoI = 0)					
Reference (MoI = 0.2)					
Reference (MoI = 0.02)					
Reference (MoI = 0.002)					
Reference (MoI = 0.0002)					
Reference (MoI = 0.00002)					
Reference (MoI = 0.000002)					
Mucus (no Virus)					
Mucus (w/ Virus)					
Mucus (treated w/ CaCl2; w/ virus)					

No cell death was observed for mucus samples without HRV, or for calcium-treated mucus samples with HRV. Untreated mucus with HRV showed partial cell death by 72 hours,

and complete cell death by 96 hours. Comparing this result to the reference standards yields similar behavior for an initial MoI of 0.00002, which translates to 100 HRV virions. Combining this value with the droplet data for untreated mucus (Chapter 4) yields an estimated 0.76 virions per droplet (or approximately 3 virions per 4 droplets).

Conclusion:

The simulated cough system was modified to include a single-stage impactor in order to collect droplets produced by cough. Such impactors were developed to analyze the number and size of airborne contaminates: they utilize inertial impaction to deposit droplets onto plates or into cell-culture media. The modifications were designed to allow the detection of pathogens transported as small droplets (which were generated via a simulated cough maneuver). Using bacteria already present within the COPD sputum as proof-of-concept, the system was shown to functionally transport these bacteria via cough-induced droplets. Additionally, calcium-treatment of the mucus successfully prevented or reduced such transport.

Viral transport was then examined by adding HRV to calcium-treated and untreated mucus and testing them within the simulated cough system. Transport was confirmed by monitoring HRV-sensitized HeLa cells for death after exposure to cough-contaminated media. Complete cell death was observed for the untreated mucus samples at 96 hours post-exposure, which corresponds to a MoI of 0.00002. No cell death was observed for calcium-treated mucus samples, indicating the successful prevention of airborne infection transmission. These data, along with the results discussed in Chapter 4, confirm the third hypothesis, indicating that airborne transmission of infectious disease can be reduced or eliminated through cationic

modification of the viscoelastic properties of mucus in such a way as to reduce or prevent droplet formation.

References:

1. Lai, S.; Wang, Y.; Wirtz, D.; Hanes, J (2008) *Adv. Drug Deliv. Rev*. 61(2): 86-100
2. Foss, S.; Keppel, J. (1999) *Resp. Care* 44(12): 1474-1485
3. Gustin, K.; Belser, J.; Wadford, D.; Pearce, M.; Katz, J.; Tumpey, T.; Maines, T. (2011) *PNAS* 108(20): 8432-8437
4. Abraham, G.; Colonno, R. (1984) *Journal of Virology* 51(2): 340-345
5. Lessler, J.; Reich, N.; Brookmeyer, R.; Perl, T.; Nelson, K.; Cummings, D. (2009) *The Lancet Journal of Infectious Diseases* 9(5); 291-300
6. jin-lab.org/wiki/research
7. Qian, J.; Hospodsky, D.; Yamamoto, N.; Nazaroff, W.; Peccia, J. (2012) *Indoor Air*doi: 10.1111/j.1600-0668.2012.00769.x
8. Yang, Y.; Sze-To, G.; Chao, C. (2012) *J. Aerosol Sci. Tech*. 46: 1-12
9. Edwards, D.; Man, J.; Brand, P.; Katstra, J.; Sommerer, K.; Stone, H.; Nardell, E.; Scheuch, G. (2004)*PNAS* 101(50): 17383-17388
10. Watanabe, W.; Thomas, M.; Clarke, R.; Klibanov, A.; Langer, R.; Katstra, K.;Fuller, G.; Griele, L.; Fiegel, J.; Edwards, D. (2007)*J Colloid Interface Sci.* 307(1): 71–78
11. Clarke, R.; Katstra, J.;Man, J.;Dehaan, W.;Edwards, D.;Griel, L. (2005)*American J Infection Control*33(5): 85
12. Duguid, J. (1946) *British Medical Journal* 265-268
13. Riley, R.; Mills, C.; O'Grady, F. (1962)*Am Rev Respir Dis* 84:511-525
14. Nalca, A.; Nichols, D. (2011) *J Gen Virol.* 92: 31-35
15. Discussions with Clarke, R.; Sung, J.; Lipp, M.; and Edwards, D.

Chapter 6: Conclusions and further work

Introduction:

The goal of this research has been to study the formation and transport of pathogen-laden droplets from the human pulmonary system, and to investigate the impact of mucus viscoelasticity on that formation. This was accomplished through the exploration of a series of related hypotheses, which were tested through the development of bench-top models for *in vitro* assessments of the relevant processes. As the role of bioaerosols in infection transmission becomes increasingly prominent, new ways of thinking about the problem and new tools for combating it are needed. The motivation behind this work is clear: to prevent airborne transmission of infectious diseases (as bioaerosols) by providing the tools necessary to reliably screen source-treatment methods.

Three hypotheses were examined:

iv) Droplet generation during tidal breathing can occur in both the upper airways (via surface shear) and lower airways (via film rupture) during inhalation, and will vary with bifurcation angle in the upper airways.

v) Mucus viscoelasticity will influence droplet formation by shear forces, with increased stiffness yielding fewer droplets in total.

vi) Reducing the number of bioaerosols generated decreases the probability of pathogen transport, and therefore the transmission of infection.

These three hypotheses were confirmed empirically, utilizing novel *in vitro* systems designed to mimic the physiological conditions of droplet generation. The first hypothesis tells us that bioaerosol formation during tidal breathing is more complex than recent published studies on expired droplets suggest, and may require treating both upper and lower airway sources, both of which can occur during inhalation. It also raises questions about the role of bioaerosols in auto-infection. The second hypothesis confirms that altering the physical properties of mucus is an effective method for reducing bioaerosol load. Finally, the third hypothesis shows that targeting bioaerosol formation can effectively prevent or reduce airborne transmission by small droplets.

The small droplet hypothesis itself was established through a review of the relevant literature, and states that small droplets (less than a few microns in diameter) are generated in the airways, and exhaled to the environment, where they may persist until they are inhaled by others. These small droplets are produced in significantly greater quantity than larger droplets, as initially reported by Papineni and Rosenthal (1997)[1], in contrast with the previously accepted notions of expelled droplets. These droplets are composed of airway lining fluid (ALF) and may contain pathogens and other material present in the airways. When inhaled, these droplets can deposit within the pulmonary system, where pathogens can establish a new infection.

Formation and transport mechanisms:

Two potential mechanisms for droplet formation were investigated: the long-held theory involving shear-induced wave-instabilities at the surface of the ALF in the upper airways, as demonstrated computationally by Moriarty and Grotberg (1999)[2]; and film rupture within expanding bronchioles in the lower airways (a process which occurs during inhalation), as

proposed by Johnson and Morawska (2009)[3]. The former is applicable to both tidal breathing and coughing. The latter has recently come to prominence due to research on expelled droplet number as a function of tidal breathing pattern, which supports the theory that droplets are formed during inhalation.

Most studies on droplet generation in the upper airways have focused on the exhalation phase of tidal breathing, however based on the experiments performed by Chowdhary et al. (1999)[4] and the computational analyses of tidal air flow in the lungs made by Green (2003)[5] and Wang et al. (2009)[6], which showed that, for tidal breathing, peak wall shear stress can occur along the inner wall directly past the first and second bifurcations during inhalation, the first hypothesis was developed. These studies indicate that droplet formation during tidal breathing in the upper airways is more likely to occur during inhalation, which not only has implications for auto-infection, but also suggests that the expelled droplet data reported by Johnson and Morawska may be applicable to both the lower and the upper airway mechanisms. Regardless, the largest number of droplets is observed during coughing, as a result of the much larger air velocities present (which increase wall shear stress and turbulence). Turbulence produces air flow velocities perpendicular to the primary airflow direction, which results in perturbations of the ALF and can drive wave-instability formation.

The droplets that are formed range in size from nanometers to microns. A brief analysis of the system indicated that convective transport of these droplets dominated diffusive transport, confirming the importance of respiration flow rates. Gravitational settling was also shown to be negligible for droplets less than a few microns in diameter. Both droplet generation mechanisms

were demonstrated to be technically feasible based on droplet size, transport and time-to-escape the lungs.

***In vitro* model development:**

To explore the proposed droplet generation mechanisms, *in vitro* models were developed, including separate systems for tidal breathing and cough air flows. These models all utilized optical particle counters (OPCs) to measure droplet size and number. Droplet generation was expected to occur in both models, although the number of droplets formed during tidal breathing was hypothesized to vary with bifurcation angle if it were an inhalation-based process. The simulated cough system was based off of research on mucus cough-clearance performed by King et al.[7], in which a pseudo-trachea was created to model upper airway conditions. This design was modified for droplet generation by Watanabe et al.[8] and further refined for the present research.

First-pass measurements of the lower and upper airway models (under tidal breathing conditions) indicated that droplets were formed through both mechanisms. Additionally droplet number dependence on bifurcation angle was observed, thus confirming the first hypothesis. The simulated cough system produced the largest number of droplets, in line with expectations. The model results were in reasonable agreement with *in vivo* data reported in the literature (when exposed interfacial area and air volume were accounted for). The threshold for tidal breathing "super-producers", as defined by Edwards et al.[9], could be met through a number of possibilities: airway geometry (bifurcation angle), number and frequency of bronchiole collapse, altered ALF physical properties or some combination of upper and lower airway mechanisms operating in tandem - the specific combination may even vary by individual.

Mucus viscoelasticity - cationic response and effect on droplet formation:

Based on the research of Edwards et al.[9] on droplet generation, as well as the work of Marriott[10] on mucus viscoelasticity, cationic treatment of mucus was used to investigate the effect of viscoelasticity on shear-driven droplet formation. The simulated cough system was chosen based on the large number of droplets produced and the expectation that the larger shear forces present during a cough represent a more strenuous test environment (and that any results should therefore carry over to the upper airway tidal breathing model). Due to the difficulty in acquiring healthy, human pulmonary mucus, several alternative sources were investigated. Based on comparisons to literature-reported viscoelastic properties of healthy mucus, COPD sputum was selected as the best choice. Published studies on the addition of cations to mucus demonstrated that altered viscoelasticity as a result. This was confirmed for the sputum samples, and used to test the second hypothesis: that the viscoelasticity of mucus would directly influence the number of droplets formed by surface shearing (specifically that increased stiffness would reduce the total number of droplets).

Salt was added in bulk to the sputum at varying concentrations and the viscoelastic properties were measured. Four salts were investigated: $CaCl_2$, $MgCl_2$, KCl, and NaCl. At low cation concentrations, a decrease in the loss tangent and an increase in the complex modulus (compared to baseline values) were observed. The effect was greater for the divalent cations (Ca, Mg) compared to the monovalent cations (K, Na). These changes indicate increased overall mucus stiffness, and confirmed that cationic exposure alters mucus viscoelasticity. However, as the concentration was increased the response was reversed and ultimately the overall stiffness decreased (the loss tangent increased while the complex modulus decreased). Increased stiffness at low cation concentrations is the result of charge-shielding, as proposed by Marriott[10], which

causes a higher entanglement density in the mucin network (an effect that was greater for divalent cations compared to monovalent cations).

Cation-treated and untreated samples were placed in the simulated cough system and the number of droplets produced was measured. Overall, increased mucus stiffness resulted in a lower total number of droplets, while decreased stiffness yielded a larger number of droplets, in confirmation of the second hypothesis.

Pathogen transport and transport prevention:

The third hypothesis stated that decreasing the total number of shear-induced droplets (through any method, including altered mucus viscoelasticity) would reduce the opportunity for pathogen transmission. A modified viable Anderson Cascade Impactor (viable-ACI) was attached to the *in vitro* cough system in order to measure pathogen transport via droplets: droplets generated in the cough system impact a petri dish (containing chocolate-agar or cell culture media) within the viable ACI, transferring any pathogens contained within.

Untreated ("neat") COPD sputum contained culturable bacteria which could be observed on agar-media plates within 48 hours (incubated). After exposure to cough-air (along with any droplets present), the petri dishes were removed from the viable-ACI, incubated for 48 hours and then observed for the presence of colony forming units (CFUs). For neat sputum, CFUs were detected in the cough-exposed plates, however for calcium-treated sputum, virtually no CFUs were seen. The calcium-treated sputum was directly plated as a control measure, and CFUs were observed at the low (isotonic) calcium concentration. Hence, bacteria were successfully transferred through the system as bioaerosols, and reduced droplet production (as a result of a cation-induced increase in mucus viscoelasticity) corresponded to reduced bacterial transport.

A similar experiment was performed with rhinovirus: the agar-media plates were replaced with plates containing cell-culture media. Untreated and treated sputum was spiked with rhinovirus at known concentrations and tested within the cough system. The cough-exposed media was then placed over rhinovirus-sensitized HeLa cells, which were observed for signs of cell-death up to 96 hours post-exposure. As a control, an untreated sputum sample with no virus added was also tested. The calcium treated sputum samples and the untreated sputum samples without virus both resulted in no observable cell death; however, for the untreated sputum sample with rhinovirus, exposed cell cultures first showed signs of death at 72 hours. Comparison to viral concentration reference data (generated from direct exposure of cells at varying virus concentrations) indicated a multiplicity of infection (MoI – ratio of virus to cells) of approximately 0.00002 for the untreated sputum samples, which indicates the initial presence of approximately 100 HRV virions (which is a little under 1 virion per droplet). This confirmed the third hypothesis.

Implications:

Taken together, the work confirmed that pathogens can be transported as bioaerosols (small droplets formed via ALF surface shearing in the upper airways); that the number of droplets formed is related to mucus viscoelasticity; and that mucus viscoelasticity can be altered by cationic addition. Tools were created to enable relatively rapid *in vitro* assessments of transmission prevention by modifying the properties of the ALF source, which was demonstrated to be an effective route for preventing pathogen transport.

As noted by Roy and Milton (2004)[11], the need for these tools and for a deeper understanding of airborne transmission in general is especially important for policy development

and design of hospitals and other public, indoor settings. There are also obvious applications in biodefense and other quarantine environments, where reducing airborne infection transmission would be of primary importance. However, there exist less critical, non-medical applications, such as particle-free laboratories, where super-producers exhaling droplets (regardless of pathogen presence) could be treated to prevent contamination of the lab environment.

Open questions:

The root cause behind super-producers remains an open question: several possible explanations were considered (upper versus lower airway sources, airway geometry, ALF physical properties), but all were demonstrated to be at least moderately feasible, and none stood out as an obvious choice. The most probable explanation is that some combination of these factors is involved, and varies from person to person and even over time for the same person, however more work is needed to further identify and isolate the individual contributing factors. Continued studies observing droplet output from the general population along with measurements of health-status and airway geometry would be needed to determine correlates between super-producers and the potential causes listed above.

Further questions remain regarding differences in the transport behavior of different pathogens. For instance, at what point does pathogen size begin to play a role? Obviously very large bacteria with sizes over a few microns are likely to simply settle out rather than remain airborne, but for pathogens less than a micron in size, is there a point at which they begin to influence droplet aerodynamics in such a way as to alter transport potential? Furthermore, does their physical structure (shape, surface proteins/filaments, etc.) play a role as well? The bench-

top models developed for this work could be used to explore a range of different pathogens (as well as specifically modified strains of those pathogens) to probe these remaining questions.

Future work:

With respect to infectious disease transmission and prevention, further research would involve several different routes. First and foremost, the transport experiments should be repeated with other bacteria and viruses – influenza, for example, would be a possible next step. This would be useful in addressing the questions posed previously regarding pathogen size and structure as well as provide further validation of the bench-top models.

Assays for more accurately quantifying the amount of bacteria or virus transported are needed to improve pathogen per droplet estimates. For example, RT-PCR might be used to measure virus concentration in cough-exposed media. This information would be useful in determining the virulence or "infectiousness" of specific pathogens when coupled to *in vivo* transmission data.

Finally, the bench-top systems should be adapted to include animal exposure models: by placing healthy animals downstream of bench-top bioaerosol sources (so as to allow exposure to contaminated airborne droplets only and prevent any other form of contact) direct airborne transmission and prevention could be observed. Existing influenza strains for different species (such as mice, pigs or ferrets) could be used to probe effects of varying breathing patterns, airway geometry and virulence.

References:

15. Papineni, R.; Rosenthal, J. (1997) *J Aerosol Med.* 10(2):105-116
16. Moriarty, J.; Grotberg, J. (1999) *J. Fluid Mech*. 397: 1–22.
17. Johnson, G.; Morawska, L. (2009)*J Aerosol Med Pulm Drug Deliv*. 22:1-9.
18. Chowdhary, R.; Singh, V.; Tattersfield, A.; Sharma, S.; Subir, K.; Gupta, A. (1999) Journal of Asthma 36(5): 419-426
19. Green, A. S. (2004) *Journal of Biomechanics* 37(5): 661-667
20. Wang, Y.; Liu, Y.; Sun, X.; Yu, S.; Gao, F. (2009) *Acta Mech Sin* 25: 737-746
21. King, M.; Brock, G.; Lundell, C. (1985) *J. Appl. Physiol.* 58: 1776-1782
22. Watanabe, W.; Thomas, M.; Clarke, R.; Klibanov, A.; Langer, R.; Katstra, K.;Fuller, G.; Griele, L.; Fiegel, J.; Edwards, D. (2007) *J Colloid Interface Sci.* 307(1): 71–78
23. Edwards, D.; Man, J.; Brand, P.; Katstra, J.; Sommerer, K.; Stone, H.; Nardell, E.; Scheuch, G. (2004)*PNAS* 101(50): 17383-17388
24. Marriott, C.; Shih, C.; Litt, M. (1979) *Biorheology* 16(4-5): 331-337
25. Roy, C.; Milton, D. (2004) *N. Engl. J. Med.* 350:1741-1744